

CA7803648

AECL-5994

**ATOMIC ENERGY  
OF CANADA LIMITED**



**L'ÉNERGIE ATOMIQUE  
DU CANADA LIMITÉE**

**ASSAY OF FISSIONABLE ISOTOPES IN AQUEOUS SOLUTION  
BY PULSED NEUTRON INTERROGATION**

by

**P. Campbell, E. M. Gardy and D. G. Boase**

**Whiteshell Nuclear Research Establishment**

**Pinawa, Manitoba, ROE 1LO**

**April 1978**

ATOMIC ENERGY OF CANADA LIMITED

ASSAY OF FISSIONABLE ISOTOPES IN AQUEOUS SOLUTION  
BY PULSED NEUTRON INTERROGATION

by

P. Campbell, E.M. Gardy and D.G. Boase

Whiteshell Nuclear Research Establishment  
Pinawa, Manitoba, R0E 1L0  
April 1978

AECL-5994

ANALYSE DES ISOTOPES FISSIBLES  
DANS UNE SOLUTION AQUEUSE PAR INVESTIGATION  
DE NEUTRONS PULSES

par

P. Campbell, E.M. Gardy et D.G. Boase

RESUME

Des analyses non-destructives de l'uranium-235 et du thorium-232 dans une solution aqueuse d'acide nitrique ont été effectuées par irradiation d'impulsions de neutrons provenant d'un générateur de neutrons Cockcroft-Walton de 14-MeV et par comptage des neutrons retardés résultant des fissions produites.

La conception du détecteur de neutrons retardés est décrite ainsi que les systèmes de comptage et de synchronisation des impulsions de neutrons. Les effets du temps d'irradiation, du temps de comptage, de la modération des neutrons, de la conception du détecteur et de la géométrie des échantillons sur la réponse des neutrons retardés de l'uranium-235 et 238 ainsi que du thorium-232, sont étudiés.

En utilisant du polyéthylène pour modérer les neutrons d'investigation, on peut analyser les solutions pour la détermination des quantités d'uranium-235 et de thorium. Des analyses comparatives effectuées avec la méthode chimique et la spectrométrie  $\gamma$  donnent des résultats satisfaisants. La méthode des neutrons est rapide et n'est pas affectée par la présence d'impuretés dans la solution, telles que du fer, du nickel, du chrome et de l'aluminium. En utilisant l'équipement expérimental décrit, les limites de détection suivantes ont été obtenues: 0.6 mg de U-235 et 9 mg de Th-232 dans un échantillon de 25 mL.

Les analyses d'échantillons hautement radioactifs peuvent être faites facilement puisque les mesures ne sont pas affectées par la présence d'un rayonnement important  $\beta$  et  $\gamma$ . Les échantillons seront enfermés dans des petits conteneurs blindés de plomb afin de protéger la personne effectuant les analyses.

Les possibilités de cette technique dans les applications d'analyses en ligne sont étudiées brèvement.

L'Energie Atomique du Canada, Limitée  
Etablissement de Recherches Nucléaires de Whiteshell  
Pinawa, Manitoba ROE 1LO  
Avril 1978

EACL-5994

ASSAY OF FISSIONABLE ISOTOPES IN AQUEOUS SOLUTION  
BY PULSED NEUTRON INTERROGATION

by

P. Campbell, E.M. Gardy and D.G. Boase

ABSTRACT

Non-destructive assay of uranium-235 and thorium-232 in aqueous nitric acid solutions has been accomplished by irradiation with pulses of neutrons from a 14-MeV Cockcroft-Walton neutron generator, and counting of the delayed neutrons emitted from the fissions induced.

Design of the delayed neutron detector assemblies is described, together with the neutron pulse timing and counting systems. The effects of irradiation time, counting time, neutron moderation, detector design and sample geometry on the delayed neutron response from uranium-235 and 238 and thorium-232 are discussed.

By using polyethylene to moderate the interrogating neutrons, solutions can be analyzed for both uranium-235 and thorium. Comparative analyses with chemical and  $\gamma$ -spectrometric methods show good agreement. The neutron method is rapid and is shown to be unaffected by the presence in solution of impurities such as iron, nickel, chromium, and aluminum. With the experimental equipment described, detection limits of 0.6 mg of  $^{235}\text{U}$  and 9 mg of  $^{232}\text{Th}$  in a sample volume of 25 mL have been achieved.

Analyses of highly radioactive samples may be done easily since the measurements are not affected by the presence of large amounts of  $\beta\gamma$  radiation. Samples can be enclosed in small lead-shielded flasks during analysis to protect the analyst.

The potential of the technique to on-line analysis applications is explored briefly.

Atomic Energy of Canada Limited  
Whiteshell Nuclear Research Establishment  
Pinawa, Manitoba, ROE 1L0  
April 1978

AECL-5994

## CONTENTS

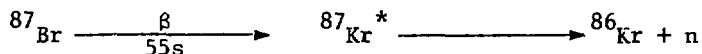
	<u>Page</u>
1. INTRODUCTION	1
2. EXPERIMENTAL	3
2.1 NEUTRON GENERATOR	3
2.2 TIMING CONTROL	4
2.3 CHOICE OF THE OPTIMUM IRRADIATION TIME	5
2.4 DETECTORS	6
2.5 NEUTRON FLUX CONTROL AND MEASUREMENT	6
3. PROCEDURE AND RESULTS	7
3.1 DETECTOR AND SAMPLE GEOMETRY	7
3.2 SENSITIVITY AND PRECISION	9
3.3 RELATIVE RESPONSE OF $^{235}\text{U}$ AND $^{232}\text{Th}$	10
3.4 EFFECT OF SOLUTION MEDIA AND SOLUTION CONTAINMENT	11
3.5 COMPARATIVE ANALYSES WITH ESTABLISHED METHODS	13
4. DISCUSSION	15
5. CONCLUSION	15
6. ACKNOWLEDGEMENTS	16
7. REFERENCES	17
TABLES	18
FIGURES	24
APPENDIX A	42

## 1. INTRODUCTION

In the nuclear industry, accurate assay of fissile and fertile materials is required for material control and accountability, and for Safeguards purposes. Non-destructive analysis techniques are prominent in this context because they are often rapid, can be used on-line, and in some cases they are insensitive to impurities which are potential interferences in conventional chemical assays. One non-destructive technique is based on pulsed neutron interrogation, in which fissions are induced in a sample by an external neutron source. The prompt or delayed neutrons, and/or gamma rays accompanying the fissions are counted and related to the quantity of the fissionable isotope in the sample.

The purpose of this work was to study the fission delayed neutron response from  $^{235}\text{U}$ ,  $^{238}\text{U}$ , and  $^{232}\text{Th}$  in nitric acid solutions, to determine the parameters which influence their response and explore the conditions in which the fissile isotopes may be differentiated from the fertile isotopes. The method developed involves irradiation of the samples with a precisely controlled series of neutron pulses from a 14-MeV neutron generator, with counting of the delayed neutrons, emitted between the pulses, for precisely controlled times.

Over 95% of the total neutrons produced from fission are prompt neutrons and are released within approximately  $10^{-10}$  s of the fission event. The delayed neutrons (0.5 to 5%) are produced by the decay of certain neutron-rich, and therefore unstable, short-lived fission product precursors. For example, one of the primary fission products,  $^{87}\text{Br}$ , decays to  $^{86}\text{Kr}$ , with the emission of a neutron as follows:



The intermediate,  $^{87}\text{Kr}$ , is formed in a highly excited state and decays almost instantaneously so that the half-life of the overall process is essentially the half-life of the  $\beta$  decay. Table 1 lists the known precursors and their half-lives<sup>(1)</sup>. The precursors are arranged according to their half-lives in six groups, designated by the half-life which best approximates the decay of the group. The yields of delayed neutrons from each group for each fissionable isotope ( $^{235}\text{U}$ ,  $^{239}\text{Pu}$ ,  $^{238}\text{U}$ ,  $^{232}\text{Th}$ ), have been extensively examined and compiled by Keepin<sup>(2)</sup> (Table 2). Differences occur in the abundance of a given group from one fissionable isotope to another and are due to differences in individual precursor yields in the fission of the different isotopes.

The delayed neutron yield counted during the interrogation of a sample is the sum of the delayed neutron yields from each fissionable isotope present. Some experimenters have used the differences in the fission properties of these isotopes to determine the quantity of each isotope present in a mixture. For example, the difference between the group abundances has been used to discriminate between the isotopes  $^{235}\text{U}$  and  $^{239}\text{Pu}$  by comparing the ratios of the abundances from group 1 and group 2 for each isotope<sup>(3)</sup>. The total yield of delayed neutrons from each isotope is also different (Table 3) and this fact too has been used to discriminate between  $^{235}\text{U}$  and  $^{239}\text{Pu}$ <sup>(4)</sup>. However, because of these differences in yields, analysis methods which do not discriminate between fissionable isotopes cannot be used for the analysis of mixtures, unless the concentration ratio of the isotopes present is known.

The delayed neutron response from a pulsed neutron irradiation, defined as the observed number of delayed neutrons produced from one gram of an isotope in one second, is a function of the length of the interrogating pulse. This effect is best demonstrated by Figures 1 and 2. Consider neutrons in group 5, which have a half-life of 0.5 s. If the counting time is 25 s (Figure 1) then after 5 s essentially all

group 5 neutron emitters have decayed and therefore they do not contribute to the count for the remaining 20 s of counting time. However, if the counting time is 0.5 s (Figure 2), group 5 activity is present during the whole counting period. Consequently, to obtain the maximum number of counts, the counting time is made approximately equal to the half-life of the species being determined. When only one isotope with a single half-life is produced, the length of the irradiation period is inconsequential because its length determines only the initial activity during the counting period and not its rate of decay. However, when a mixture of isotopes of different half-lives is produced, the length of the irradiating period is important. Figure 1 illustrates that an irradiation period which is longer than the half-life of the species to be counted causes shorter-lived species to reach saturation, while the longer half-life species continue to increase in activity. Thus even if a counting period equal to the half-life of the short-lived species was used, the activity from the longer-lived species would dominate the counting period. In summary, to make a particular precursor dominant during the decay period, the irradiation and counting periods are made approximately equal to the half-life of that precursor.

## 2. EXPERIMENTAL

### 2.1 NEUTRON GENERATOR

The irradiation source used was a neutron generator\* of the Cockroft-Walton type<sup>(5)</sup> producing 14-MeV neutrons by the  ${}^2\text{H}({}^3\text{H},n){}^4\text{He}$  reaction. A schematic of the experimental arrangement is shown in Figure 3. Pulses of 14-MeV neutrons are produced by electrostatic

---

\* Manufactured by Accelerators Incorporated, Austin, Texas



deflection of the positive ion beam both before and after the accelerating tube, and by systematic interruption of the power to the radio-frequency ion source. The high voltage terminal of the generator is insulated from the main chassis and the only hard wire connection to the terminal is from the high voltage transformer. Since the high voltage terminal operates the accelerating voltage (150 kV), while the chassis, including the last electrode of the accelerating column, is at ground potential, the pulse control signals to the high voltage terminal from the control console must be conveyed by an electrically non-conducting route. In the original instrument design, the signals for the pre-acceleration and radiofrequency pulsing were transmitted via a microwave link, but this unit was not reliable and required considerable maintenance. We therefore designed an optical link (Figure 4) which conveys pulses of light to a light-sensitive transistor located in the high voltage terminal. This system is simple and has proved to be reliable.

The maximum flux achieved by this generator is  $7 \times 10^{10}$  neutrons  $s^{-1}$ . The flux decays with a half-life of about 30 min during continuous operation at a beam current of 1 mA and a potential of 100 kV, and the useful life of a target is about 2.5 mA.h. As the deuterons impinge on the target, some are absorbed in the copper-titanium substrate and the reaction  ${}^2\text{H}({}^2\text{H},n){}^3\text{He}$ , which produces 3-MeV neutrons, becomes possible. The longer the target is irradiated the more probable is this reaction, until after about 2 mA.h the 3-MeV component is a significant portion of the interrogating flux.

## 2.2 TIMING CONTROL

The timing unit which controls the counting and neutron generator pulsing systems was developed in our laboratories and is described in a separate report<sup>(6)</sup>. The desired irradiation pulse time (illustrated by A-B in Figure 5a) is selected on the timing control. This automatically sets the counting period (D-E) equal to the irradiation period and

the "gating-on" of the preamplifiers, to  $\sim 1$  ms after the generator pulse ceases. This prevents saturation of the preamplifiers by the large number of pulses produced in the detection system by the 14-MeV neutrons. A second delay (C-D) is used between the preamplifier switching on and the counting period to prevent the preamplifier switching noise from occurring in the counting period. The delay periods are the same for all irradiation times selected. A further short delay (E-F) is used at the end of each counting period to prevent over-lap between counting and the next irradiation period. The irradiation-counting sequence is continued until a preset number of cycles has been completed. The counts from all cycles are summed and printed out to complete one experiment. For the analyses described later, each experiment was repeated until sufficient data were obtained for statistical analysis, usually four to nine times.

### 2.3 CHOICE OF THE OPTIMUM IRRADIATION TIME

Table 2 lists the abundance and half-lives of each delayed neutron group for some isotopes of uranium, plutonium and thorium. In each case, the most abundant neutron group is group 4. Thus, from the previous discussion of the variation of observed yield with irradiation and counting times, an irradiation period equal to the half-life of group 4, approximately two seconds, should offer the optimum yield. However, since contributions to the total delayed neutron response arise from the other five groups, a more rigorous analysis is required to obtain the optimum irradiation time. Appendix 1 gives details of this analysis and provides an equation which relates the delayed neutron response to the irradiation times, taking into account the six groups of precursors with different half-lives and abundances. The result is:

$$R(n,T) = F\beta\bar{\nu} \left[ \sum_{i=1}^6 \left( \frac{a_i}{\lambda_i} (1 - e^{-\lambda_i T/2n}) \right) (1 - e^{-\lambda_i (T-\delta)/2n}) e^{-\lambda_i \delta} \sum_{z=0}^{n-1} (n-z) e^{-\lambda_i ZT/n} \right]$$

All terms are defined in Appendix 1.  $R(n,T)$  is the delayed neutron response from  $n$  irradiation and counting cycles in  $T$  seconds, where the irradiation and counting times are equal. To deduce the optimum irradiation-counting time, the ratio of the response from  $n$  cycles in time  $T$  to the response from one cycle in time  $T$ , is plotted against the number of cycles,  $n$ . An example is given in Figure 7 for uranium-235. When  $T = 50$  s, the optimum response is obtained using 40 or more cycles, which corresponds to an irradiation pulse time of 0.6 s or less. For our work, a pulse length of 0.5 s was selected.

#### 2.4 DETECTORS

Two types of detection unit were used. Twelve helium-3 gas proportional detectors\* were placed in a rectangular slab, or in an annulus, of polyethylene. The auxiliary electronics were the same for both units. High voltage (1800 volts D.C.) was supplied to all the detectors connected in parallel. Two parallel counting systems, each monitoring six detectors, were used. Each counting system consisted of a gated preamplifier, an amplifier, a single channel analyser and a scaler (Figure 3). Gated preamplifiers<sup>(7)</sup> were required since the interrogating flux produces a large number of pulses in the helium-3 detectors which saturate the preamplifier electronics. The gating, directed by the timing control unit, diverted the signals from the detectors to ground during the neutron pulse. Figure 6 is a schematic showing the distribution of the D.C. voltage to the detection units. To maintain a stable detector output, the values of the resistors and/or capacitors were carefully matched to the detectors.

#### 2.5 NEUTRON FLUX CONTROL AND MEASUREMENT

The interrogating flux could be approximately controlled by maintaining the generator operating parameters at preset values. This

---

\* Texlum Detectors, Texas Nuclear Corp., Austin, Texas

control is not sufficiently precise for the analysis measurements required, since it does not allow for the loss of tritium from the target during deuteron bombardment. Consequently, the interrogating flux is continuously monitored by a 14-MeV neutron detector<sup>(8)</sup> in which alpha particles produced in the reaction  $^{12}\text{C}(n,n')3\alpha$  in a carbon foil cause scintillations in a zinc sulfide layer. The scintillations are detected by a photomultiplier tube and counted during the irradiation period. The threshold energy for this reaction is 8 MeV and thus essentially only the 14-MeV neutrons are detected. Any scattered neutrons, or 3-MeV neutrons produced by the  $^2\text{H}(^2\text{H},n)^3\text{He}$  reaction, will not be detected. The counts recorded by the 14-MeV neutron detector are used to normalize the interrogating flux falling on the sample and permit correction of each analysis for changes in the interrogating flux.

### 3. PROCEDURE AND RESULTS

#### 3.1 DETECTOR AND SAMPLE GEOMETRY

Initial experiments were conducted using the slab detector. Solutions of uranyl nitrate were assayed in square plastic sample containers of various thicknesses. At a sample thickness of 5 mm, the calibration curve began to depart significantly from linearity at a uranium concentration of about  $100 \text{ g.L}^{-1}$  (Figure 8). The analysis precision at  $100 \text{ g.L}^{-1}$  was  $\pm 10 \text{ g.L}^{-1}$  ( $2\sigma$ ). The detection limit was equivalent to 2.5 g of  $^{238}\text{U}$ . The effect of increasing thicknesses of the water phase on the moderation and attenuation of the delayed neutrons was studied most conveniently by placing water-filled sample containers of different thicknesses between a piece of  $^{235}\text{U}$  metal and the slab detector. These tests showed that up to 5 mm of water did not attenuate the delayed neutrons emitted by  $^{235}\text{U}$ , but greater thicknesses reduced

the delayed neutron response. For example, a 10-mm aqueous layer caused 22% attenuation.

In subsequent tests, the sample container used was a 45-mL tube (25-mm diameter) which was rotated about its vertical axis at about 45 revolutions per minute. This sample geometry was chosen so that the sample volume, and the neutron attenuation effects, could be reduced. The neutron response versus concentration curve, given in Figure 9, was linear up to approximately  $180 \text{ g.L}^{-1}$  and the detection limit was reduced to 1 g of  $^{238}\text{U}$ .

The effect of various thicknesses of polyethylene moderator between the sample and the helium-3 detectors on the detection efficiency was studied. Neutron emitting sources of americium/lithium and plutonium/beryllium replaced the sample in these tests. Figure 10(a) shows that the helium-3 detector response increased as the thickness of polyethylene increased, while Figure 10(b) shows the response decreased with increasing distance between the helium-3 detector and the neutron emitter, with no polyethylene present. The combination of these results suggested that an optimum response would be obtained with 50 mm of polyethylene between the neutron source (or sample) and the detectors. All the detectors would be the same distance from the source. Thus a cylindrical array of detectors embedded in an annulus of polyethylene was constructed for subsequent work.

Two cylindrical well detectors were manufactured. Because of the limited availability of materials, the first contained only 25 mm of polyethylene between the sample cavity and the detectors. The cavity was also lined with 1-mm thick cadmium. The second unit had 50 mm of polyethylene between sample and detectors and could be placed around the neutron generator target, to permit a minimum distance between the sample, the target and the detectors. Figures 11 and 12 depict the two detection units, named the "small" and "large", well detectors respectively.

The effects of rotating the sample, and changing the sample container diameter, were studied using each well detector. When the sample was rotated at 3500 r/s the response of the small detector was the same for all containers of less than 25-mm diameter (Figure 13). For larger diameter vessels the response decreased as a function of the diameter. For the corresponding stationary vessels, the response was lower and decreased with increasing diameter as shown in Figure 13. The increase in response due to rotation was about 25% and was probably due to the greater area of sample presented to the interrogating beam, and also to the detector. Using the large detector, sample rotation had no effect on the delayed neutron response. In this case the detectors and the moderator surround the sample, and the interrogating neutrons, being scattered, entered the sample from all directions.

### 3.2 SENSITIVITY AND PRECISION

The standard solutions used in this work were prepared from depleted  $U_3O_8$ ,  $^{235}U$  metal and  $ThO_2$  dissolved in nitric acid. The calibration curves were checked on each occasion whenever the generator was used after being shut down for several hours. The day-to-day reproducibility of the calibration curve was noted over the lifetime of a tritium target. From five calibration runs, the slope of the thorium curve was determined to be  $65 \pm 3.5$  counts  $g^{-1}.s^{-1}$  (equivalent to a precision of  $\pm 5.4\%$  ( $2\sigma$ )). Each standard solution was assayed up to nine times and the precision of a single assay was 4 to 5% ( $2\sigma$ ). Each point on the calibration curve was the mean of several determinations of each standard. The precision ( $2\sigma$ ) for a typical sample with an unknown concentration of the isotope under investigation was  $\pm 3.6\%$ .

Solutions of natural and enriched uranium and thorium in nitric acid were irradiated with pulses of 14-MeV neutrons of 0.5 s and 50 s duration. The sample vessel was a 25 mL, 25-mm diameter polyethylene vial. The delayed neutron counts were accumulated for 100 cycles for

0.5 s pulsing, and 1 cycle for 50 s pulsing, in each experiment to illustrate the effects of different pulse lengths. Up to nine experimental runs were made on each sample. Figures 14 and 15 show the calibration curves for both well detectors. The best detection limits for the small detector were: 50 mg uranium-235, 250 mg thorium-232, and 150 mg uranium-238; while for the large detector they were: 0.6 mg uranium-235, 9 mg thorium-232 and 6.25 mg uranium-238.

### 3.3 RELATIVE RESPONSE OF $^{235}\text{U}$ AND $^{232}\text{Th}$

The large detector exhibited an enhanced response for  $^{235}\text{U}$  relative to  $^{232}\text{Th}$ . The theoretical response ratio,  $^{235}\text{U}/^{232}\text{Th}$ , calculated using 14-MeV cross sections and fast fission delayed neutron abundances, is 4:1. The experimentally observed ratio was 36:1. Since the fission cross section for  $^{235}\text{U}$  increases with decreasing energy, particularly in the 100 eV to thermal region, a fraction of the 14-MeV neutrons must, therefore, have been moderated in the polyethylene or the aqueous solution. The principal moderation was shown to have occurred in the polyethylene surrounding the helium-3 detectors since, on placing the sample and the generator target head outside of the detector block, the  $^{235}\text{U}/^{232}\text{Th}$  response ratio decreased to the unmoderated value of four. With the target and sample in the original configuration, as shown in Figure 12, and with the diameter of the sample vessel reduced by half, the response ratio was again 36:1. Thus no significant moderation had occurred in the sample medium.

For thorium the threshold energy for fission is about 1 MeV and the fission cross section is highest for 14-MeV neutrons. When a thorium solution was irradiated with a cadmium liner in the detector, the response was 10% lower than in the absence of cadmium, showing that some thermalization of the delayed neutrons had occurred in the aqueous sample.

To increase the thermalization of the interrogating neutrons in order to exploit the higher  $^{235}\text{U}$  response, a block of polyethylene was inserted between the sample and the target head. Figure 16a shows that the delayed neutron response from a  $^{235}\text{U}$  solution increased with an increasing thickness of the polyethylene block up to about 35 mm. There was also a countervailing decrease of response with increasing distance between target and sample, and the latter became predominant at target to sample distances greater than 35 mm. This is illustrated by the first two curves in Figure 16a. In tests where the solution was covered with a cadmium thermal neutron absorber, the polyethylene had no effect on the delayed neutron response. As would be expected, for a  $^{232}\text{Th}$  solution, no effect of the polyethylene, over that caused by the increased target to sample distance, was detected (Figure 16b). The ratio of the delayed neutron responses for  $^{235}\text{U}$  and  $^{232}\text{Th}$  increased linearly with increasing polyethylene thickness between the target head and sample. The maximum value obtained was 930:1 with a 106-mm polyethylene spacer.

The energy spectrum of the interrogating neutrons was also affected by the 3-MeV neutrons produced from the  $^2\text{H}(^2\text{H},n)^3\text{He}$  reaction. Since the 14-MeV neutron detector does not respond to 3-MeV neutrons, they were not included in the interrogating flux measurement, or in the normalization ratio used to adjust sample measurements. However, the 3-MeV neutrons do cause fast fission in the specimens under test and thus the value of the calibration slope increased with target exposure time. The effect was most noticeable with the smaller cadmium-lined well detector. The problem was adequately resolved by repeating the calibration procedure more frequently when targets of more than a few mA.h exposure were in use.

#### 3.4 EFFECT OF SOLUTION MEDIA AND SOLUTION CONTAINMENT

In addition to the effects of sample thickness and geometry previously discussed, other variables such as sample density, and neutron-



emitting reactions other than fission, were expected to influence the observed delayed neutron yield from aqueous solutions of uranium and thorium. Moderation of the interrogating neutrons may be influenced by the presence of hydrogen and other light elements. Delayed neutrons are produced by the neutron reaction  $^{16}\text{C}(n,\gamma)^{17}\text{N}$ , in the polyethylene detector annulus and in the sample vessel, and from the  $^{17}\text{O}(n,p)^{17}\text{N}$  reaction in the aqueous solutions.

With the experimental arrangement described, it was found that the neutron reactions described resulted in a background contribution of only 30 neutron-counts  $\text{s}^{-1}$  in the large detector, and the necessary corrections to sample measurements could be readily applied.

The effects of solution media changes were examined using a series of  $0.5 \text{ mol.L}^{-1}$  aqueous thorium, and uranium-235 solutions in 1 to  $9 \text{ mol.L}^{-1}$  nitric acid. No statistically significant change was observed in the delayed neutron response over this acid concentration range. However, with a  $0.5 \text{ mol.L}^{-1}$  thorium nitrate solution in 30% tributyl phosphate -70% diethyl benzene, the delayed neutron response was 18% lower than for the corresponding aqueous solution. Thus some knowledge of the nature of the medium of samples to be analyzed is necessary. Other common elements such as aluminum, chromium, nickel, and iron could be expected to occur in samples requiring analysis. Tests, using thorium nitrate solutions, to which  $170 \text{ g.L}^{-1}$  ferrous sulphate,  $9 \text{ g.L}^{-1}$  aluminum nitrate,  $16 \text{ g.L}^{-1}$  nickel and  $10 \text{ g.L}^{-1}$  chromium were added, showed these elements had no effect on the delayed neutron response (Table 4).

Since this freedom from interferences suggests that the procedure could be applied to on-line analyses of impure liquors containing fissionable materials, specimen solutions contained in a polyethylene vial, covered with 3.2-mm thick steel to simulate containment in a steel pipe, were assayed. The analyses were not affected by the presence of the steel.

In further tests, samples were assayed in the presence of a 1.48 GBq  $\gamma$  source of cesium-137. Again the analyses were not affected, demonstrating that the method can be directly applied to solutions containing fission products which arise in irradiated fuel reprocessing operations. In the experimental apparatus described, it is desirable, however, that highly radioactive solutions should be contained in a shielded container to minimize exposure to the analyst during sample transfers. This can be accomplished by enclosing the sample vial in a suitable lead shield. Tests with samples contained in a 5-mm thick lead container showed that the analyses were not statistically different from those carried out in unshielded vessels.

A simple simulated test of the on-line analysis of a flowing solution was also set up as shown in Figure 17. A flowing aqueous stream of thorium nitrate was assayed by irradiating the solution with 0.50 pulses of 14-MeV neutrons. The optimum flowrate conditions were determined for this particular experiment. The assay precision determined for thorium was  $\pm 15 \text{ g.L}^{-1}$ .

### 3.5 COMPARATIVE ANALYSES WITH ESTABLISHED METHODS

To test the validity and applicability of the method discussed, samples of uranium and thorium in nitric acid solutions were taken from a laboratory solvent-extraction process in operation at Whiteshell Nuclear Research Establishment (WNRE) to recover  $^{235}\text{U}$  from residues arising from the manufacture of  $\text{ThO}_2/\text{UO}_2$  fuels. Samples were analysed by delayed neutron, chemical, and gamma spectroscopy methods and the results compared.

To discriminate between uranium and thorium the principles described earlier, in which the interrogating neutrons are moderated by polyethylene, were utilized. The sample was first assayed for uranium

using a 106-mm polyethylene spacer. For the samples tested, the delayed neutron yield was thus essentially due to the fissile  $^{235}\text{U}$  component. The  $^{235}\text{U}$  concentration in each sample was calculated from a calibration curve established on the same day. When the polyethylene spacer was removed and the target was placed immediately adjacent to the cadmium covered sample, the delayed neutron response was due to both uranium and thorium. Calibration curves for both uranium and thorium were established for this arrangement using separate standard solutions. The uranium concentration, determined from the first series of measurements, was used to correct the second combined assay, thus permitting the thorium concentration to be calculated.

Uranium-235 was assayed in seventy-three samples which contained uranium at concentrations in the range  $< 0.5$  to  $14.4 \text{ g.L}^{-1}$  and thorium in the range  $< 0.1$  to  $400 \text{ g.L}^{-1}$ . The  $^{235}\text{U}$  results were in good agreement with the gamma spectroscopy values, with a mean difference of less than one per cent. Table 5 presents some typical results.

For the chemical analysis for thorium two methods were available. The first, an EDTA titration procedure<sup>(9)</sup>, was subject to interferences by iron, aluminum and nickel in the samples. As previously described, the neutron method is not influenced by these elements and it therefore offers advantages over the titrimetric procedure. The second chemical method, a colorimetric procedure using Thoron<sup>(10)</sup> is also free of interferences from the elements listed, and was therefore used for comparative analyses with the neutron method. The results are given in Table 6. In general the agreement shown is within the precision of the two methods. However, the chemical colorimetric procedure is not ideally suited to these analyses since dilution of the samples to the working range of the method ( $10$  to  $100 \text{ mg.L}^{-1}$ ) was required, and an improved analysis precision is desirable for an intercomparison with the delayed neutron procedure.

#### 4. DISCUSSION

The neutron method described is capable of rapid, precise analyses of aqueous and solvent samples containing uranium-235 and/or thorium-232. A single analysis can be performed in 10 minutes, after setting up the neutron generator. It is thus economical where large numbers of samples of similar composition are to be analyzed. Samples require a minimum pretreatment and are subsequently available for other analyses if desired. Further, since the presence of large amounts of  $\beta\gamma$  radiation can be tolerated and the samples can be analyzed while contained in a small lead flask, the procedure is directly applicable to liquors from fuel reprocessing streams, without resorting to shielded facilities and remote chemical handling or separation procedures. Where the number of samples to be analyzed per day is small, the method may not be economical since the neutron generator may require up to two hours to bring into operation and to complete calibration.

#### 5. CONCLUSION

Solutions containing uranium and thorium have been successfully analysed using a pulsed neutron interrogation technique. Based on repetitive analyses of standard solutions the precision of the technique is better than 5% ( $2\sigma$ ) with a detection limit of 0.6 mg  $^{235}\text{U}$  and 9 mg of  $^{232}\text{Th}$ . The technique has been shown to be insensitive to some changes in the solution media, including large amounts of non-fissionable elements which commonly interfere in direct chemical analysis procedures. Enhancement of the delayed neutron response of the fissile isotopes present, and discrimination of the fissile from the fertile nuclides present, is achieved by moderating the interrogating 14-MeV neutrons with appropriate

amounts of polyethylene. The method is non-destructive and is not affected by the presence of large amounts of  $\beta\gamma$  activity in the sample. The requirement for  $\beta\gamma$  shielded analysis facilities may therefore be reduced. Comparative analyses with established chemical and gamma spectrometric methods show good agreement. The neutron method offers a significant increase in speed over the chemical procedures for thorium. It also offers potential for application to on-line analysis. In this case a more suitable neutron source would be a compact isotopic source such as americium/lithium, plutonium-238/beryllium or californium-252. This application needs further study to establish the sensitivity and precision which can be achieved.

## 6. ACKNOWLEDGEMENTS

The authors wish to acknowledge the technical assistance of I.M. Smith and J.E. Swiddle, the mechanical and electronic maintenance shops of WNRE, and their colleagues in the Analytical Science Branch who provided the chemical analyses.

## 7. REFERENCES

1. R.J. Tuttle, Nucl. Sci. Eng. 56, 37 (1975).
2. G.R. Keepin, Physics of Nuclear Kinetics, Addison Wesley (1965).
3. B.P. Maksyutenko, Yu. F. Balakshev, V.I. Bulanenko, G.I. Zhdanova, and A.A. Shimanskii, Soviet Atomic Energy 39, 1078 (1975).
4. J.M. Jamieson and G.G. Eichholz, Trans. Am. Nuc. Soc. 23, 96 (1976).
5. J.D. Cockcroft and E.T.S. Walton, Proc. Roy. Soc. (London) A136, 619 (1932).
6. J.E. Swiddle, Unpublished information, Whiteshell Nuclear Research Establishment (1977).
7. L.V. East, Nucl. Instrum. and Methods 71, 328 (1969).
8. C.A. Feu Alvim and A.N. Dos Santos, Nucl. Instrum. and Methods 105, 289 (1972).
9. A. Bruch and K.F. Lauer, "Precise compleximetric determination of thorium", Commission of the European Communities report, EUR-4714e (1971).
10. M.H. Fletcher, F.S. Grimaldi and L.B. Jenkins, Anal. Chem. 29, 963 (1957).

TABLE 1

KNOWN DELAYED NEUTRON PRECURSORS & HALF LIVES<sup>(1)</sup>

Group	Group Half-Life (s)	Precursor	Individual Half-Life (s)
1	55	<sup>87</sup> Br	55.7
2	22	<sup>88</sup> Br	15.9
		<sup>136</sup> Te	21
		<sup>137</sup> I	24.6
		<sup>141</sup> Cs	25
3	6	<sup>134</sup> Sb	11
		<sup>84</sup> As	5.6
		<sup>87</sup> Sc	5.8
		<sup>89</sup> Br	4.5
		<sup>82</sup> Rb	4.5
		<sup>93</sup> Rb	5.9
		<sup>137</sup> Te	3.5
		<sup>138</sup> I	6.5
4	2	<sup>85</sup> As	2.0
		<sup>88</sup> Se	1.5
		<sup>90</sup> Br	1.6
		<sup>92</sup> Kr	1.8
		<sup>93</sup> Kr	1.2
		<sup>94</sup> Rb	2.7
		<sup>135</sup> Sb	1.7
		<sup>139</sup> I	2.6
		<sup>142</sup> Xe	1.2
		<sup>142</sup> Cs	1.9
		<sup>143</sup> Cs	1.7
		<sup>144</sup> Cs	1.1
5	0.5	<sup>86</sup> As	0.9
		<sup>89</sup> Se	0.4
		<sup>91</sup> Br	0.6
		<sup>95</sup> Rb	0.36
		<sup>99,98</sup> Y	0.35, 0.8
		<sup>140</sup> I	0.86
		<sup>145</sup> Cs	0.6
6	0.2	<sup>92</sup> Br	0.25
		<sup>96</sup> Rb	0.20
		<sup>97</sup> Rb	0.17

TABLE 2

DELAYED NEUTRON HALF LIVES, DECAY CONSTANTS AND  
YIELDS FROM FAST FISSION<sup>(2)</sup>

Group Index, i	Half-Life (s)	Decay Constant $\lambda_i$ , s <sup>-1</sup>	Relative Abundance $a_i$
<sup>235</sup> U (99.9% 235)			
1	54.51 ± 0.94	0.0127 ± 0.0002	0.038 ± 0.003
2	21.84 ± 0.54	0.0317 ± 0.0008	0.213 ± 0.005
3	6.00 ± 0.17	0.115 ± 0.003	0.188 ± 0.016
4	2.23 ± 0.06	0.311 ± 0.008	0.407 ± 0.007
5	0.496 ± 0.029	1.40 ± 0.081	0.128 ± 0.008
6	0.179 ± 0.017	3.87 ± 0.369	0.026 ± 0.003
<sup>238</sup> U (99.98% 238)			
1	52.38 ± 1.29	0.0132 ± 0.0003	0.013 ± 0.001
2	21.58 ± 0.39	0.0321 ± 0.0006	0.137 ± 0.002
3	5.00 ± 0.19	0.139 ± 0.005	0.162 ± 0.020
4	1.93 ± 0.07	0.358 ± 0.014	0.388 ± 0.012
5	0.490 ± 0.023	1.41 ± 0.067	0.225 ± 0.013
6	0.172 ± 0.009	4.02 ± 0.214	0.075 ± 0.005
<sup>239</sup> Pu (99.8% 239)			
1	53.75 ± 0.95	0.0129 ± 0.0002	0.038 ± 0.003
2	22.29 ± 0.36	0.0311 ± 0.0005	0.280 ± 0.004
3	5.19 ± 0.12	0.134 ± 0.003	0.216 ± 0.018
4	2.09 ± 0.08	0.331 ± 0.012	0.328 ± 0.010
5	0.549 ± 0.049	1.26 ± 0.115	0.103 ± 0.009
6	0.216 ± 0.017	3.21 ± 0.255	0.035 ± 0.005
<sup>232</sup> Th (100% 232)			
1	56.03 ± 0.95	0.0124 ± 0.0002	0.034 ± 0.002
2	20.75 ± 0.66	0.0334 ± 0.0011	0.150 ± 0.005
3	5.74 ± 0.24	0.121 ± 0.005	0.155 ± 0.021
4	2.16 ± 0.08	0.321 ± 0.011	0.446 ± 0.015
5	0.571 ± 0.042	1.21 ± 0.090	0.172 ± 0.013
6	0.211 ± 0.019	3.29 ± 0.297	0.043 ± 0.006



TABLE 3

ABSOLUTE TOTAL DELAYED NEUTRON YIELD PER FISSION

Isotope	Delayed Neutron Yield per Fission	
	Fast Fission	Thermal Fission
$^{239}\text{Pu}$	0.0063	0.0061
$^{233}\text{U}$	0.0070	0.0066
$^{240}\text{Pu}$	0.0088	-
$^{235}\text{U}$	0.0165	0.0154
$^{238}\text{U}$	0.0412	0.0158
$^{232}\text{Th}$	0.0496	-

TABLE 4

THE EFFECT OF FOREIGN IONS ON THE NEUTRON ASSAY  
OF THORIUM SOLUTIONS

Delayed Neutron Response From Standard Sample	Standard Sample Plus Foreign Ion	Foreign Ion (mol.L <sup>-1</sup> )
207 ± 16	206 ± 10	0.625 (Fe)
32.2 ± 1.2	32.4 ± 2.5	0.28 (Ni)
32.2 ± 1.2	32.4 ± 1.6	0.185 (Cr)
59 ± 3	60 ± 2	0.105 (Al)
59 ± 3	62 ± 2	0.511 (Al)
202 ± 12	193 ± 10	5 (HNO <sub>3</sub> )

TABLE 5

COMPARATIVE ANALYSES OF URANIUM-235 IN PROCESS  
SAMPLES - BY THE DELAYED NEUTRON AND GAMMA  
SPECTROMETRIC METHODS

Sample Identification	Known Thorium Concentration (g.L <sup>-1</sup> )	Uranium by Gamma Spectrometry (g.L <sup>-1</sup> )	Uranium by Delayed Neutron (g.L <sup>-1</sup> ) (2σ=5%)
10-C-2	376	12.9	13.7
10-F1-R	424	15.9	15.5
10-D-2	245	8.7	8.2
10-MS-F3	379	13.8	13.8
10-F-2	392	13.9	13.7
10-MS-R3	296	2.9	2.9
10-P1	< 0.1	10.9	10.9
10-MS-R2	297	1.3	1.4
10-C1	245	9.6	9.4
10-D1	184	6.8	6.8
9-MS-F2	394	12.0	12.1
9-MS-U3	0.2	5.7	5.6
9-P1	< 0.1	16.0	15.8
9-C1	401	12.3	12.0
9-D1	218	7.0	6.9
9-MS-F1	393	11.9	11.6
			Mean Difference = 0.8%

TABLE 6

COMPARISON OF THORIUM ASSAYS BY NEUTRON AND  
THE CHEMICAL THORON METHOD

Sample Identification	Delayed Neutron ( $2\sigma=5\%$ ) g.L <sup>-1</sup>	Chemical g.L <sup>-1</sup> ( $2\sigma=3\%$ )	Difference %
9-MS-R3	215	199	+ 7.4
9-MS-R2	268	259	+ 3.4
9-MS-R1	275	271	+ 1.5
9-MS-F3	274	271	+ 1.1
9-R1	259	256	+ 1.2
10-C2	333	338	- 1.5
10-F1-R	424	424	0
10-D-2	229	237	- 3.5
10-MS-F-3	372	361	+ 3.0
10-F2	372	368	+ 1.1
10-MS-R3	281	277	+ 1.4
10-C1	245	221	+ 9.8
10-MS-F4	290	296	- 2.1
10-D1	184	191	- 3.8
10-MS-F1	358	368	- 2.7
10-MS-F2	364	371	- 1.9
10-MS-F5	285	296	- 3.9
			Mean Difference 0.5%

DELAYED NEUTRONS FROM 1 GRAM URANIUM -235

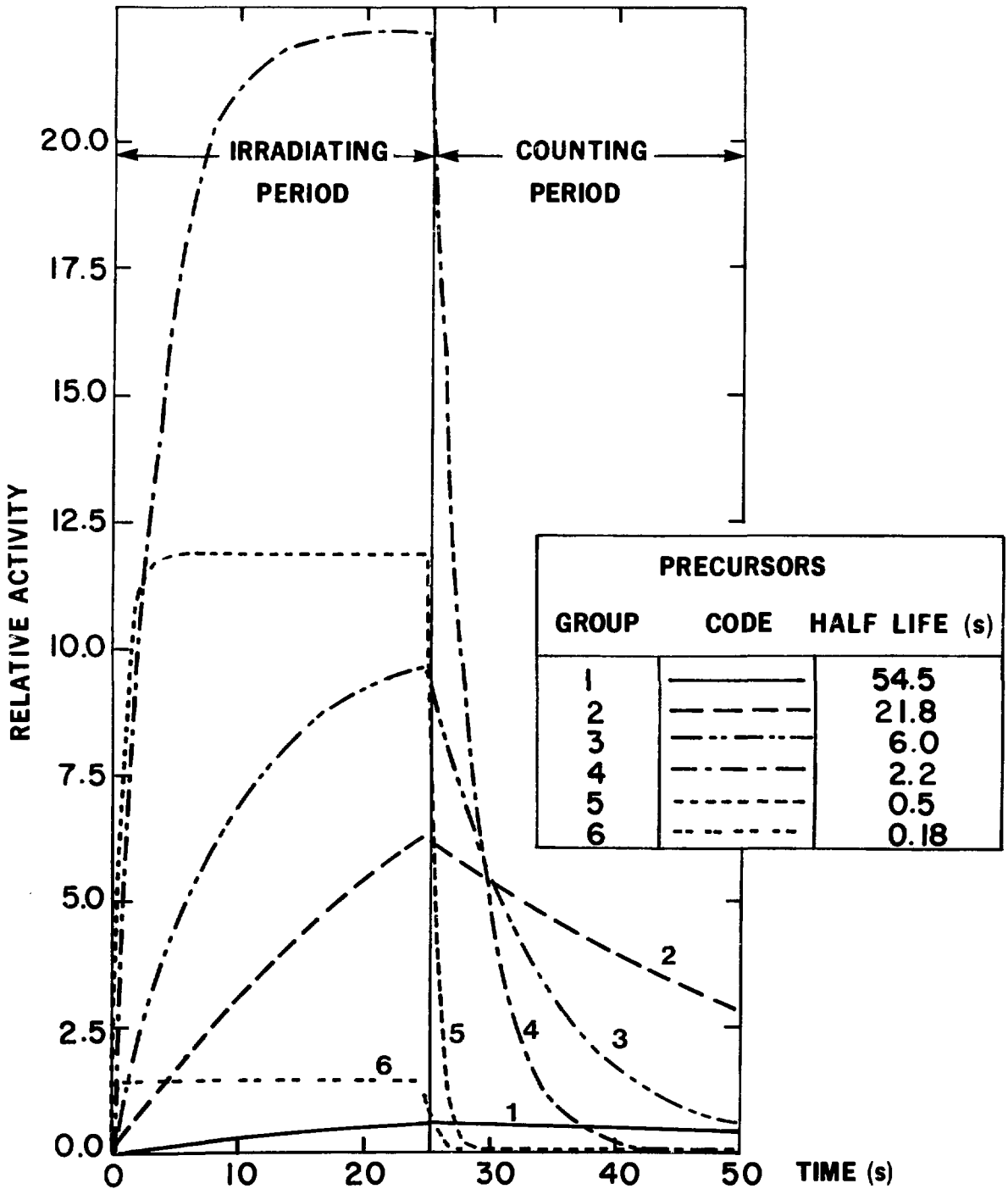
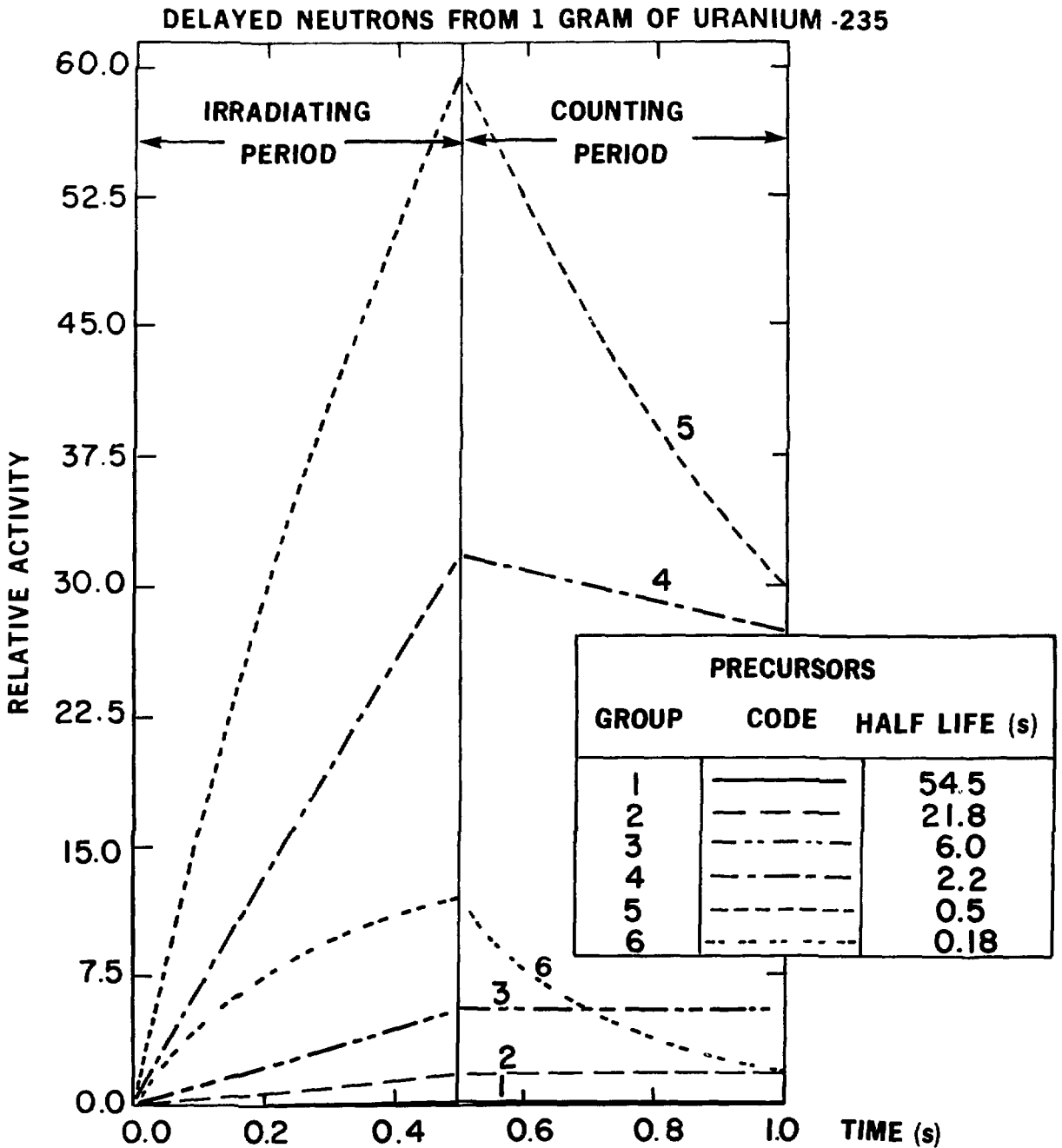


FIGURE 1

THE RELATIVE ACTIVITY GROWTH AND DECAY CURVES OF PRECURSOR GROUPS PRODUCED BY A 25s IRRADIATION



**FIGURE 2**  
**THE RELATIVE ACTIVITY GROWTH AND DECAY CURVES OF**  
**PRECURSOR GROUPS PRODUCED BY 0.5s IRRADIATION**

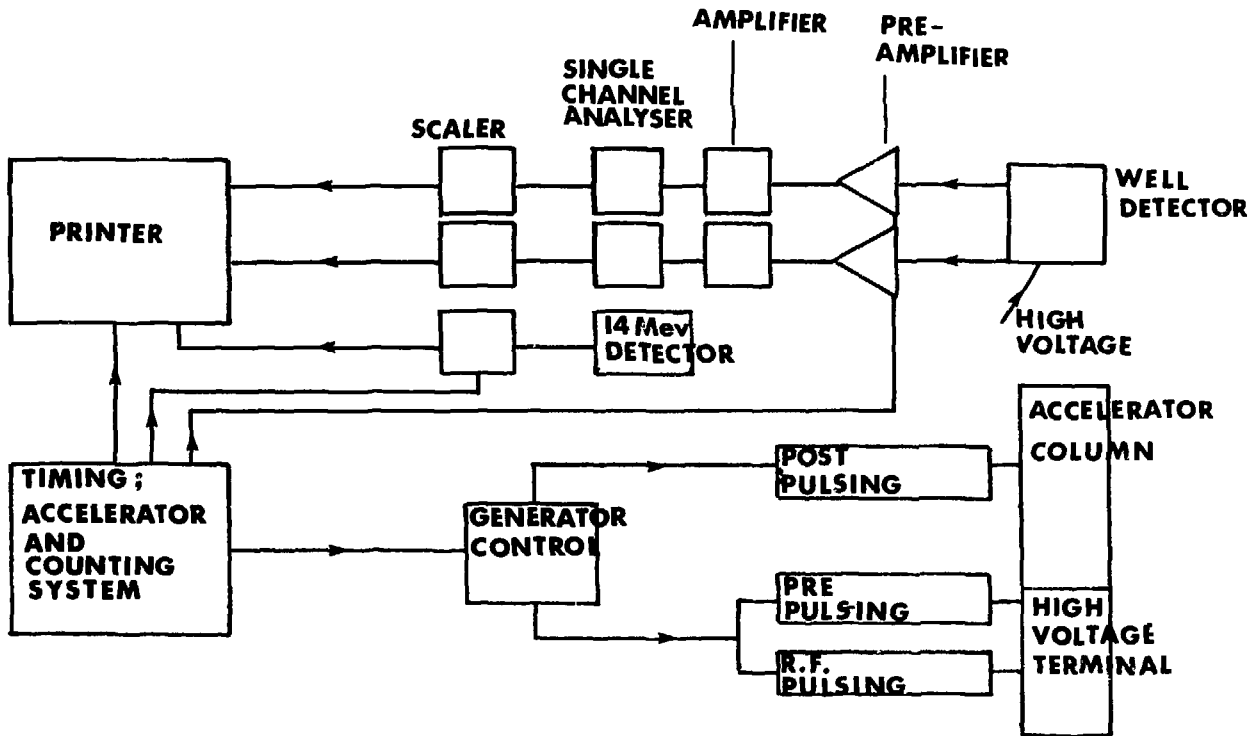


FIGURE 3

NEUTRON GENERATOR EXPERIMENTAL SYSTEM

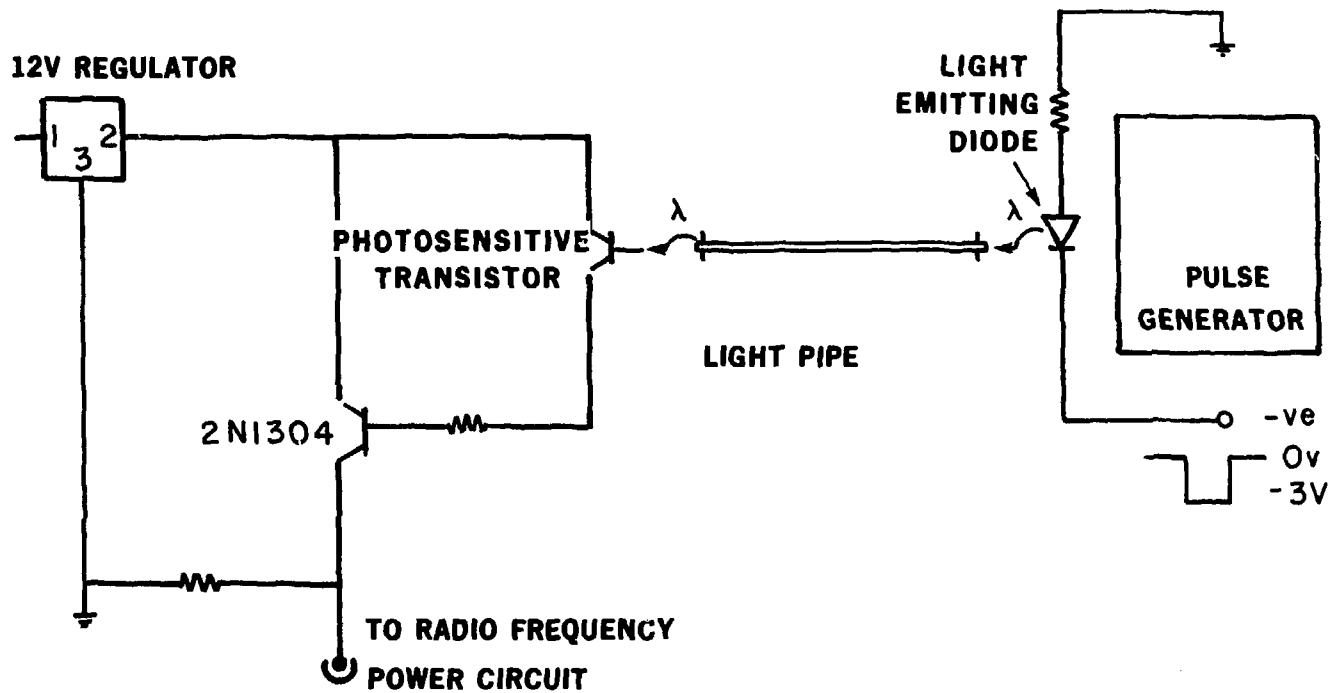
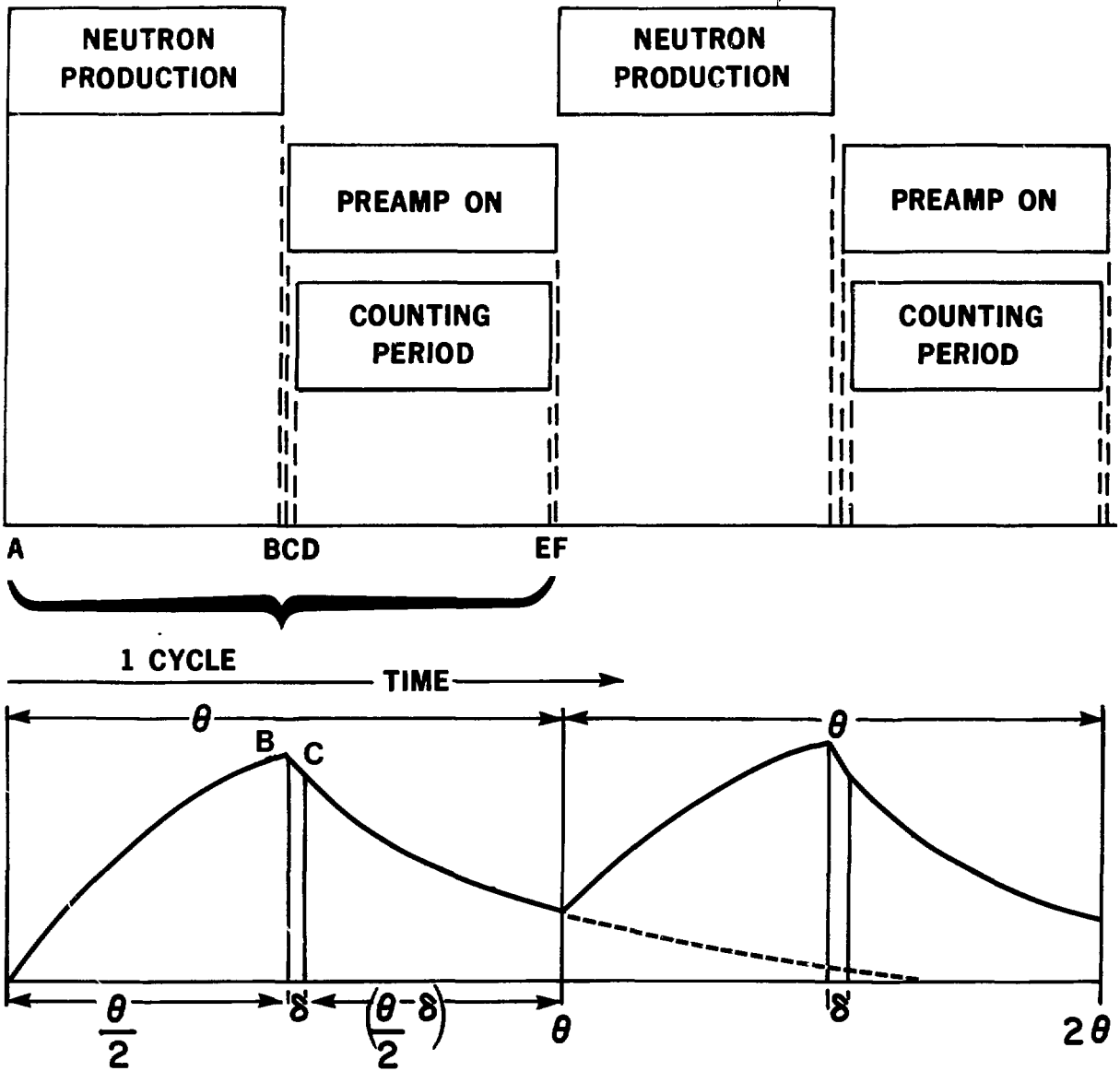


FIGURE 4

SCHEMATIC FOR R.F. GRID PULSING SYSTEM





**FIGURE 5**  
**EXPERIMENTAL TIMING SEQUENCE AND DELAYED NEUTRON PRODUCTION**  
**AND DELAY CURVES FOR TWO IRRADIATION/COUNTING CYCLES**

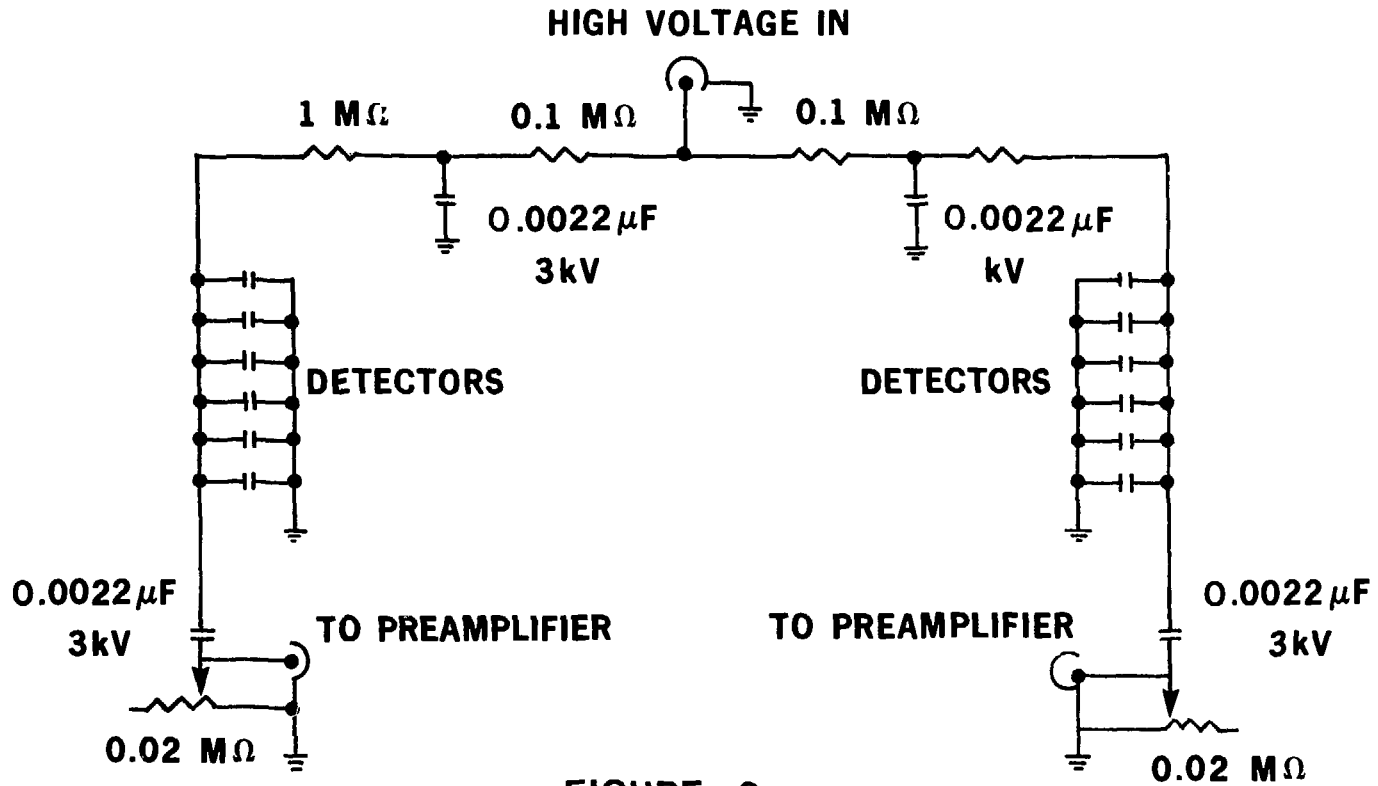


**FIGURE 6**  
**HIGH VOLTAGE DIVIDER NETWORK FOR TWO BANKS**  
**OF SIX HELIUM-3 DETECTORS**

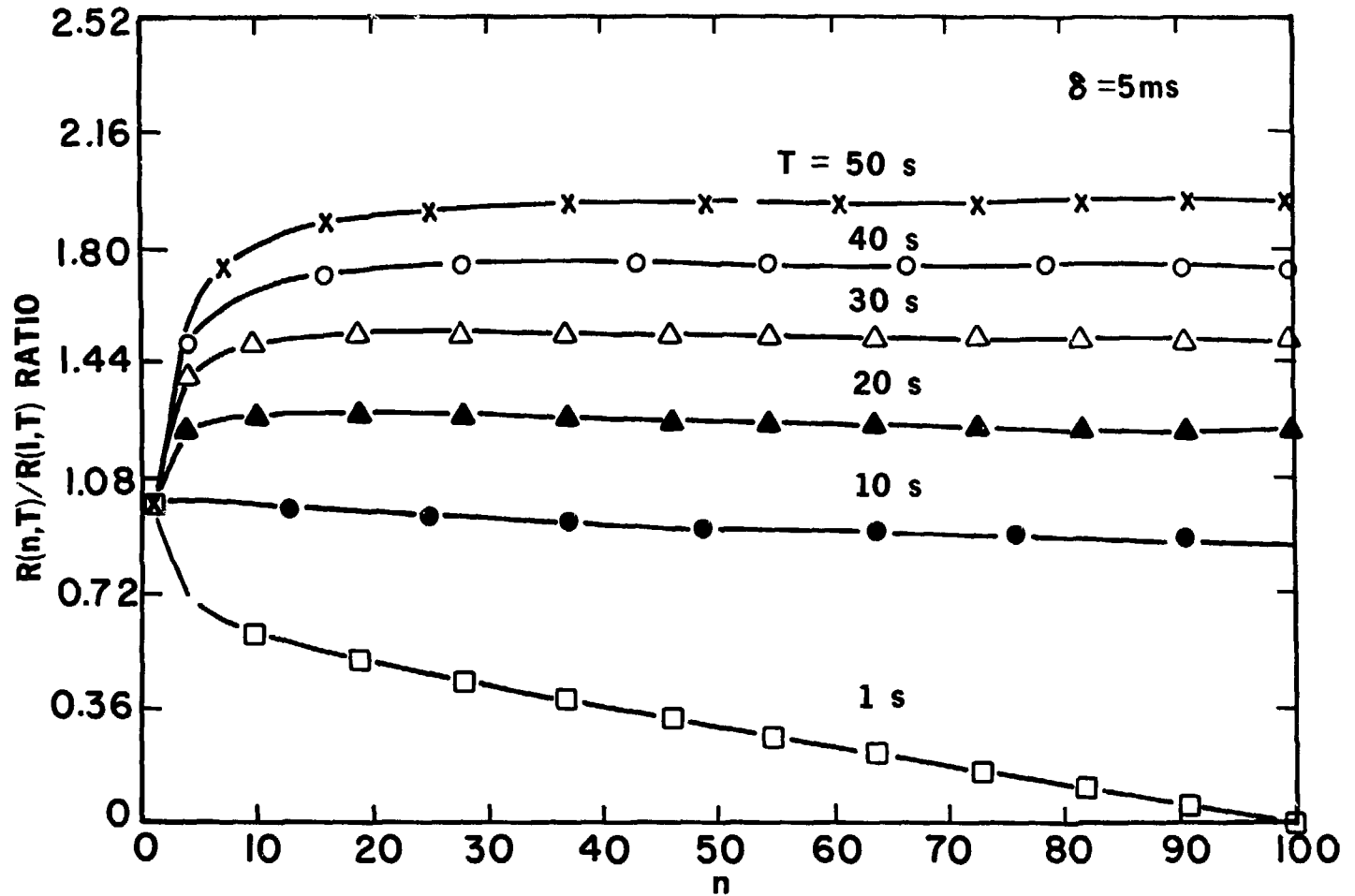
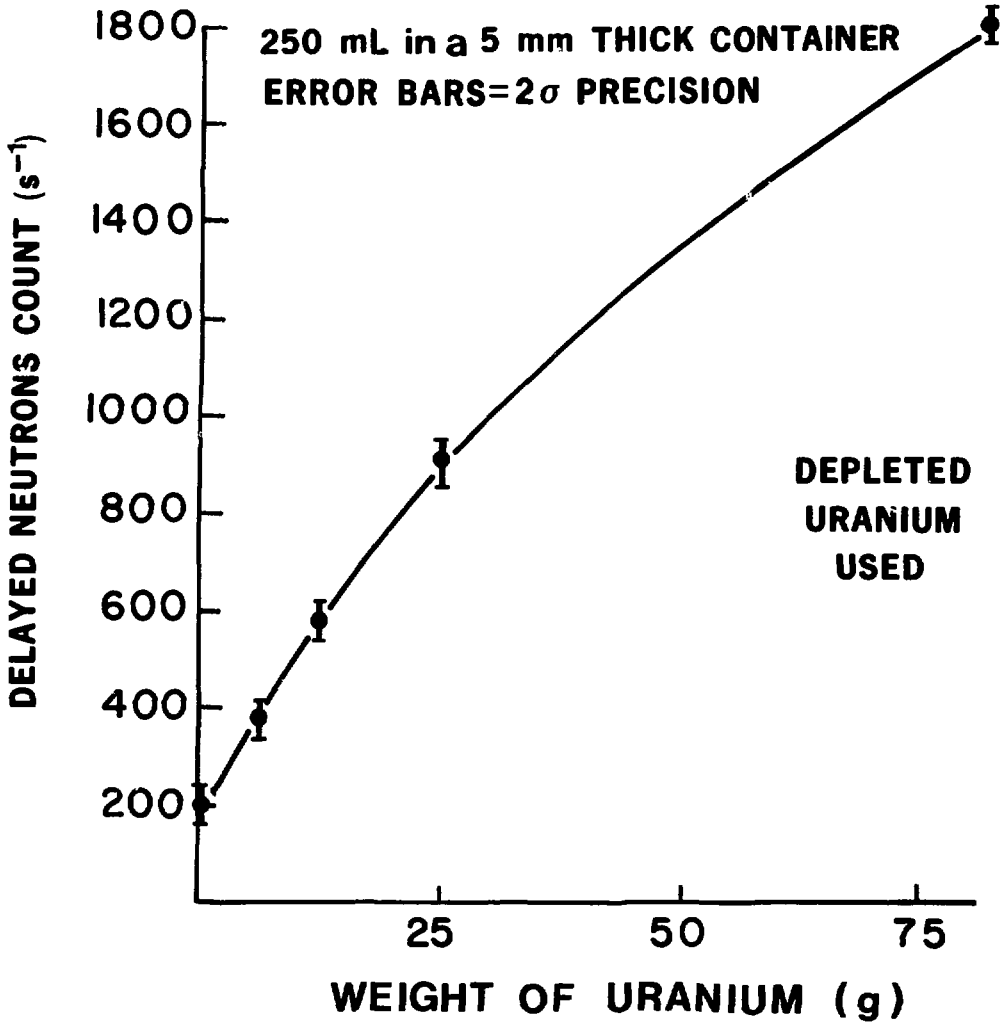
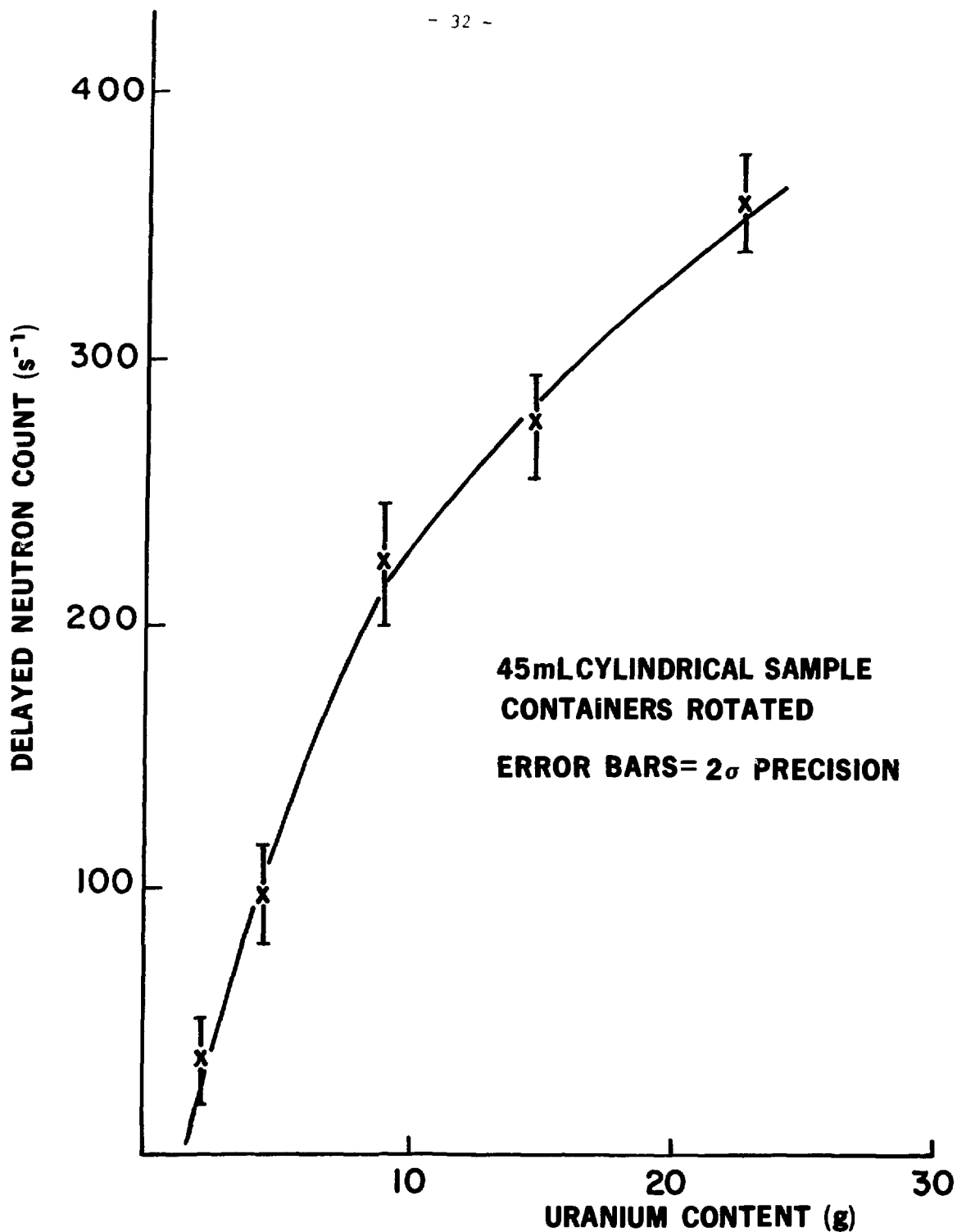


FIGURE 7 THE RATIO OF DELAYED NEUTRON RESPONSE FOR  $n$  CYCLES IN TOTAL TIME  $T$  TO ONE CYCLE IN TIME  $T$  VERSUS THE NUMBER OF CYCLES,  $n$ , FOR 1g OF  $^{235}\text{U}$



**FIGURE 8**  
**DELAYED NEUTRON RESPONSE FROM AQUEOUS URANYL**  
**NITRATE SOLUTIONS USING THE SLAB DETECTOR**



**FIGURE 9**  
**ASSAY OF URANYL NITRATE SOLUTIONS USING SLAB**  
**DETECTOR**

POSITION OF SOURCE  
AT ALL TIMES

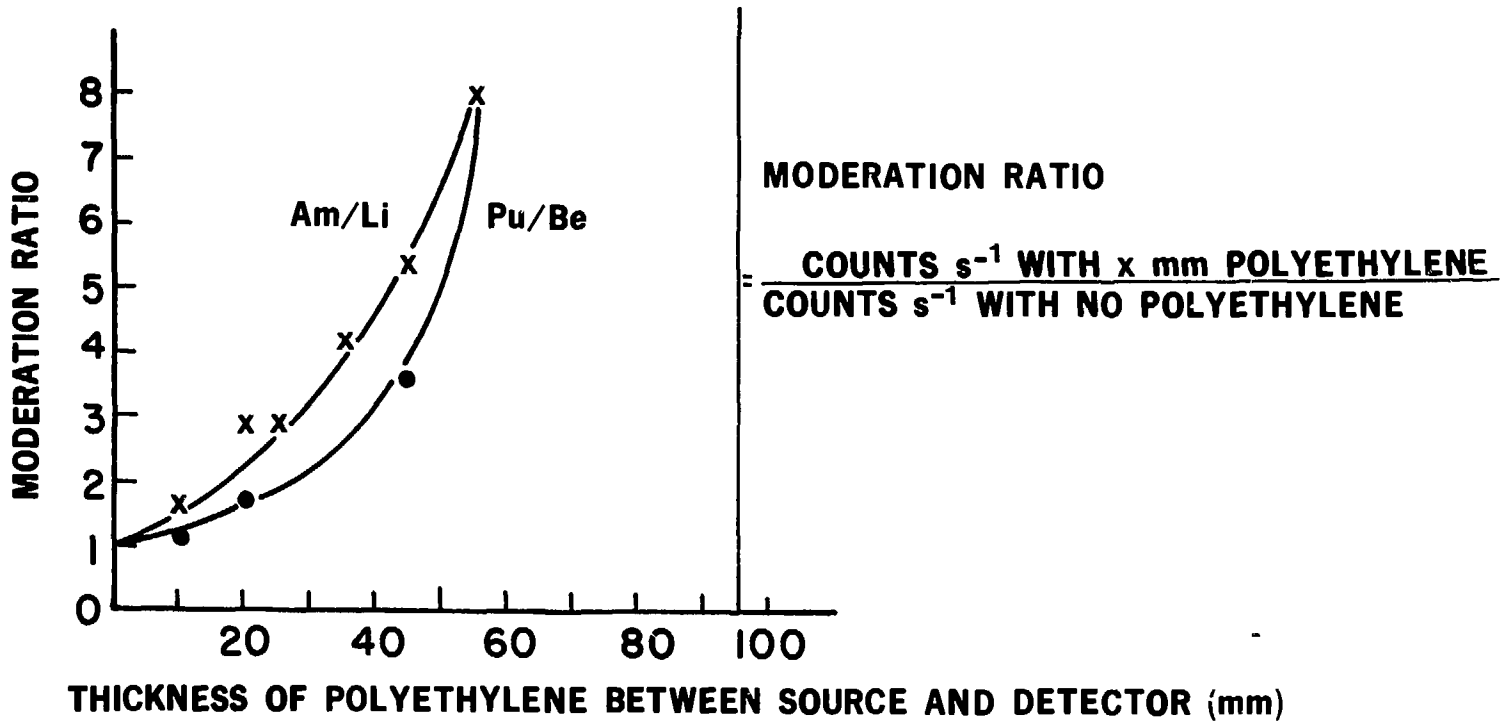
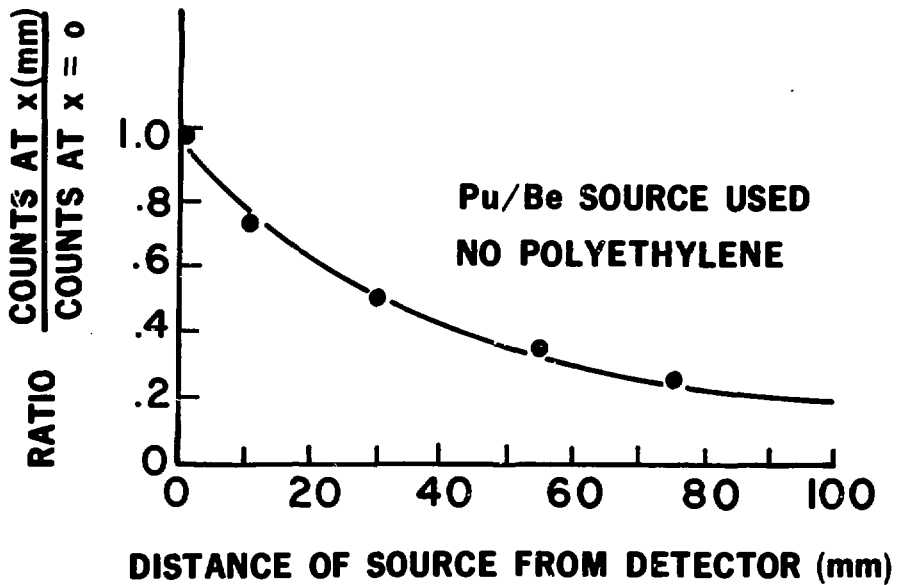
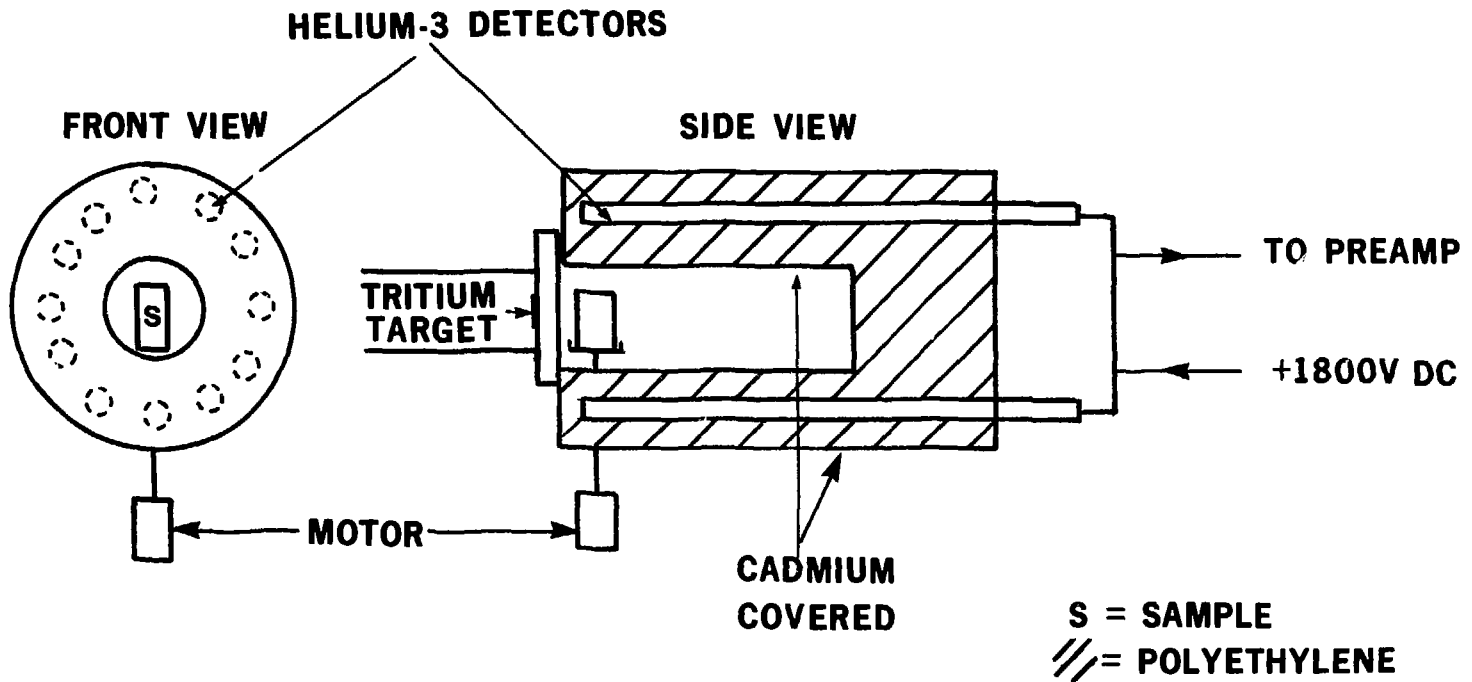


FIGURE 10(a)

THE EFFECT OF POLYETHYLENE MODERATION ON THE RESPONSE OF A HELIUM-3  
DETECTOR TO ISOTOPIC NEUTRON SOURCES



**FIGURE 10(b)**  
**THE EFFECT OF DISTANCE BETWEEN SOURCE**  
**AND DETECTOR ON THE RESPONSE OF THE**  
**HELIUM-3 DETECTOR**



**FIGURE 11**  
**'SMALL' WELL DETECTOR**



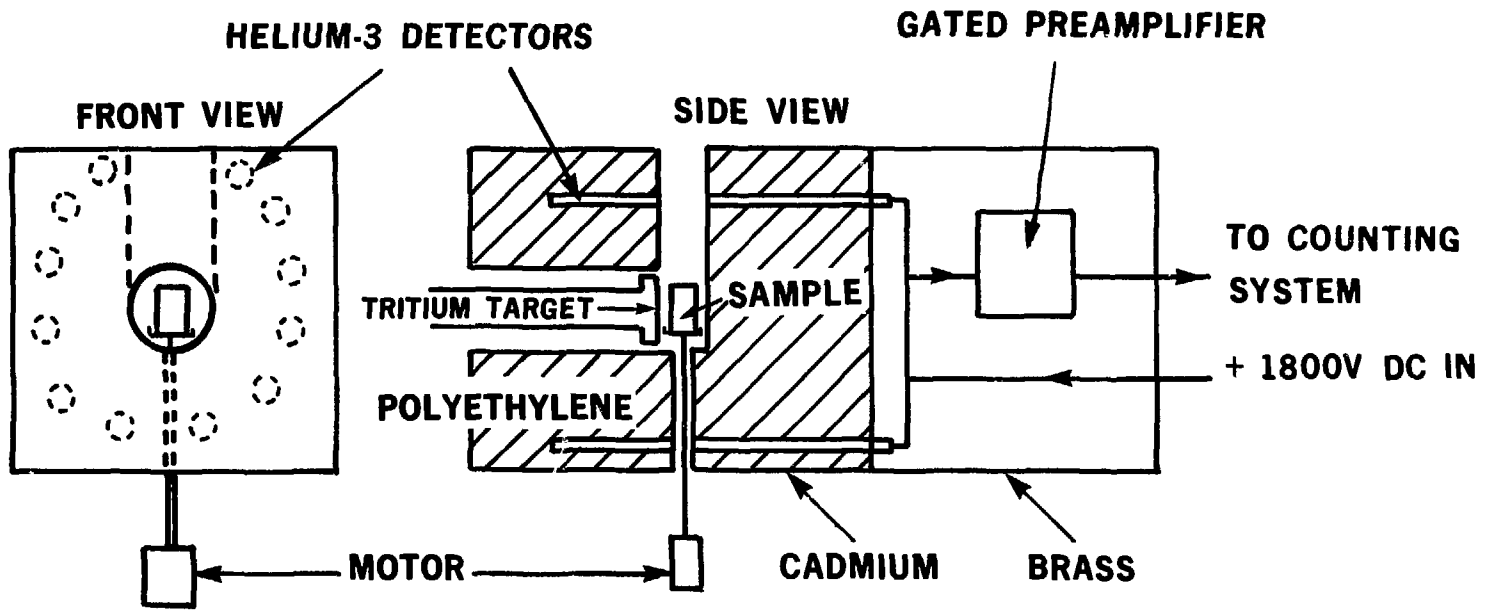


**FIGURE 12**  
**'LARGE' WELL DETECTOR**

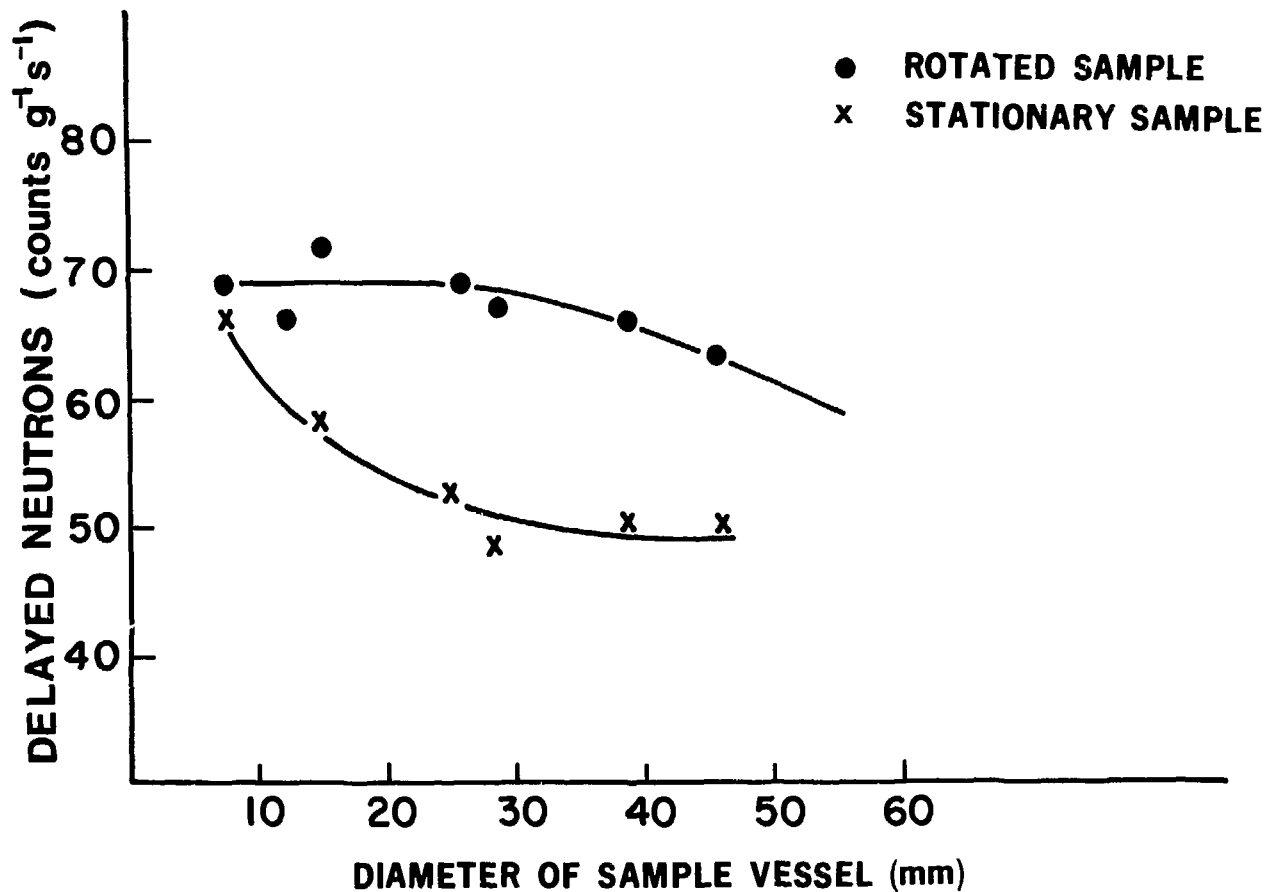


**FIGURE 13**  
**THE EFFECT OF SAMPLE DIAMETER AND SAMPLE ROTATION ON THE DELAYED NEUTRON RESPONSE OF THE SMALL DETECTOR**

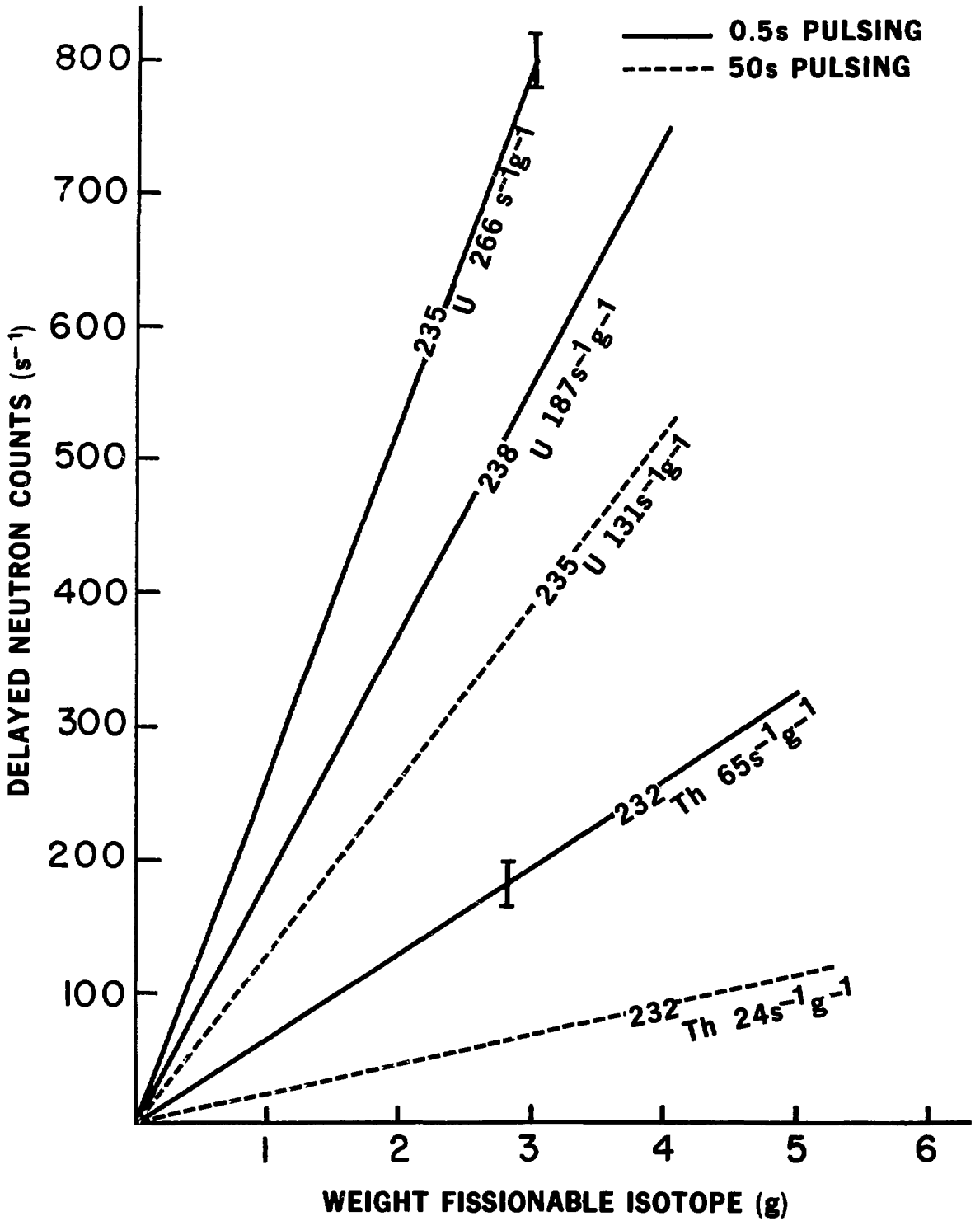


FIGURE 14  
DELAYED NEUTRON YIELDS FOR CADMIUM LINED SMALL DETECTOR

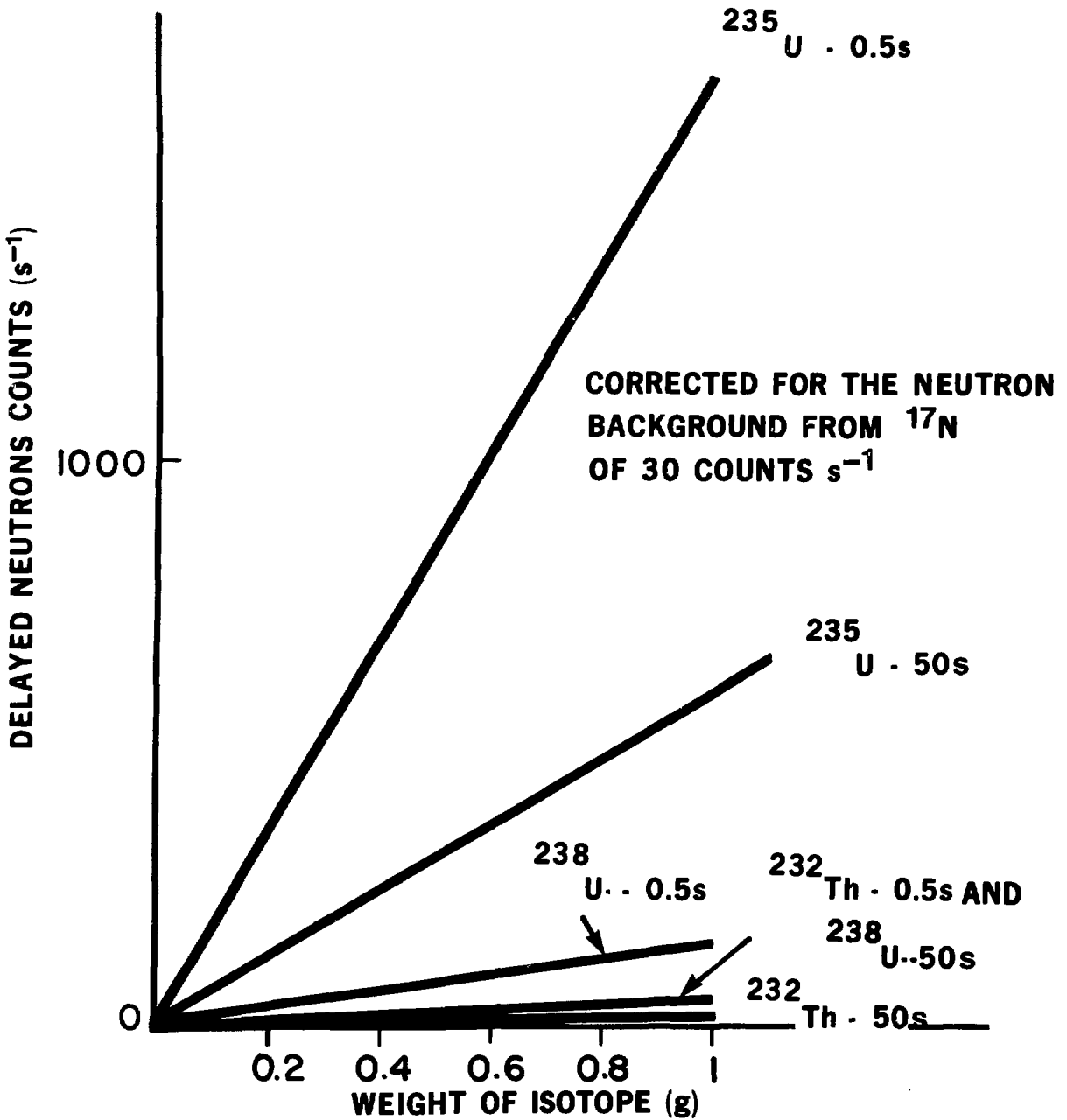


FIGURE 15  
CALIBRATION CURVES FOR SOME FISSIONABLE ISOTOPES  
AT TWO PULSING TIMES USING THE LARGE DETECTOR

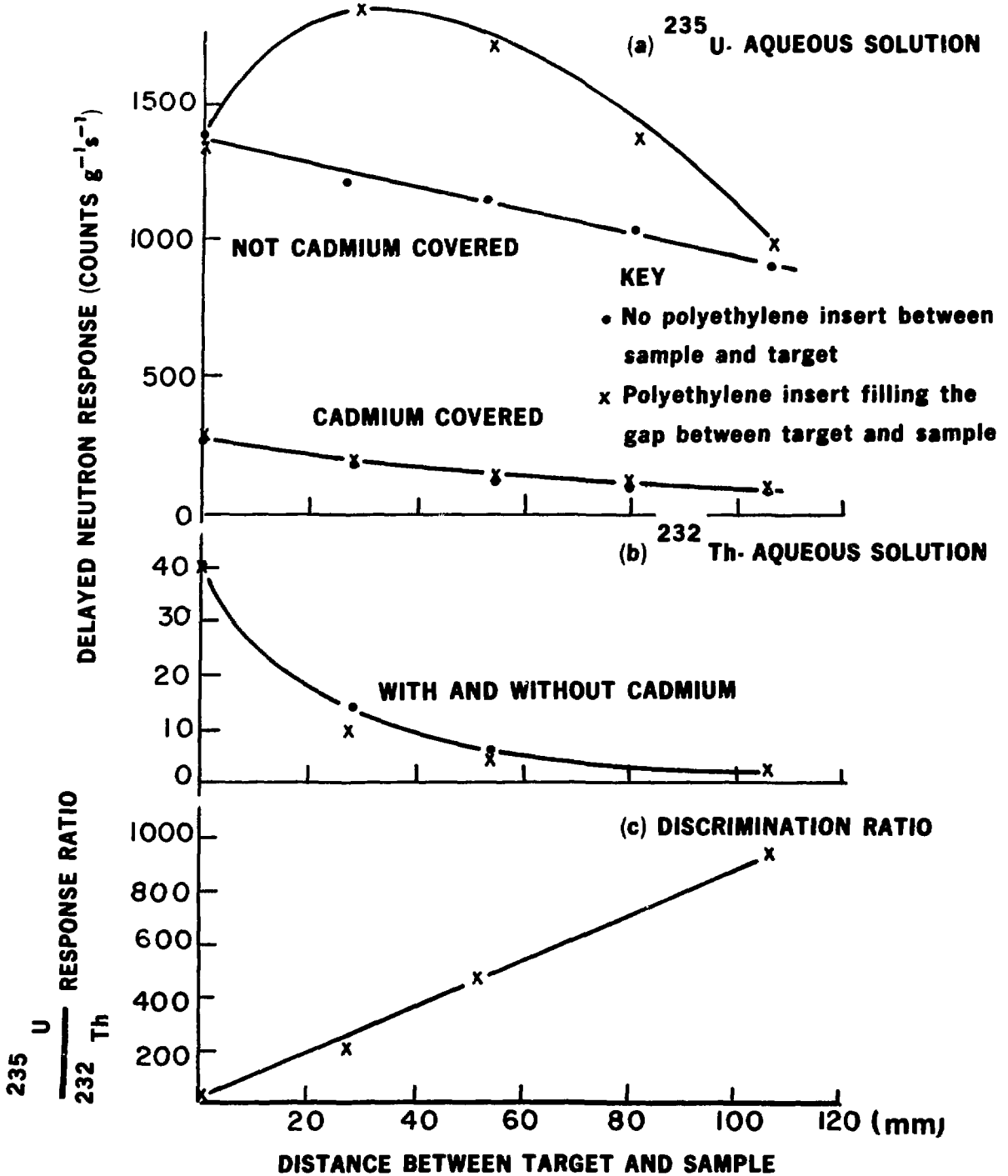
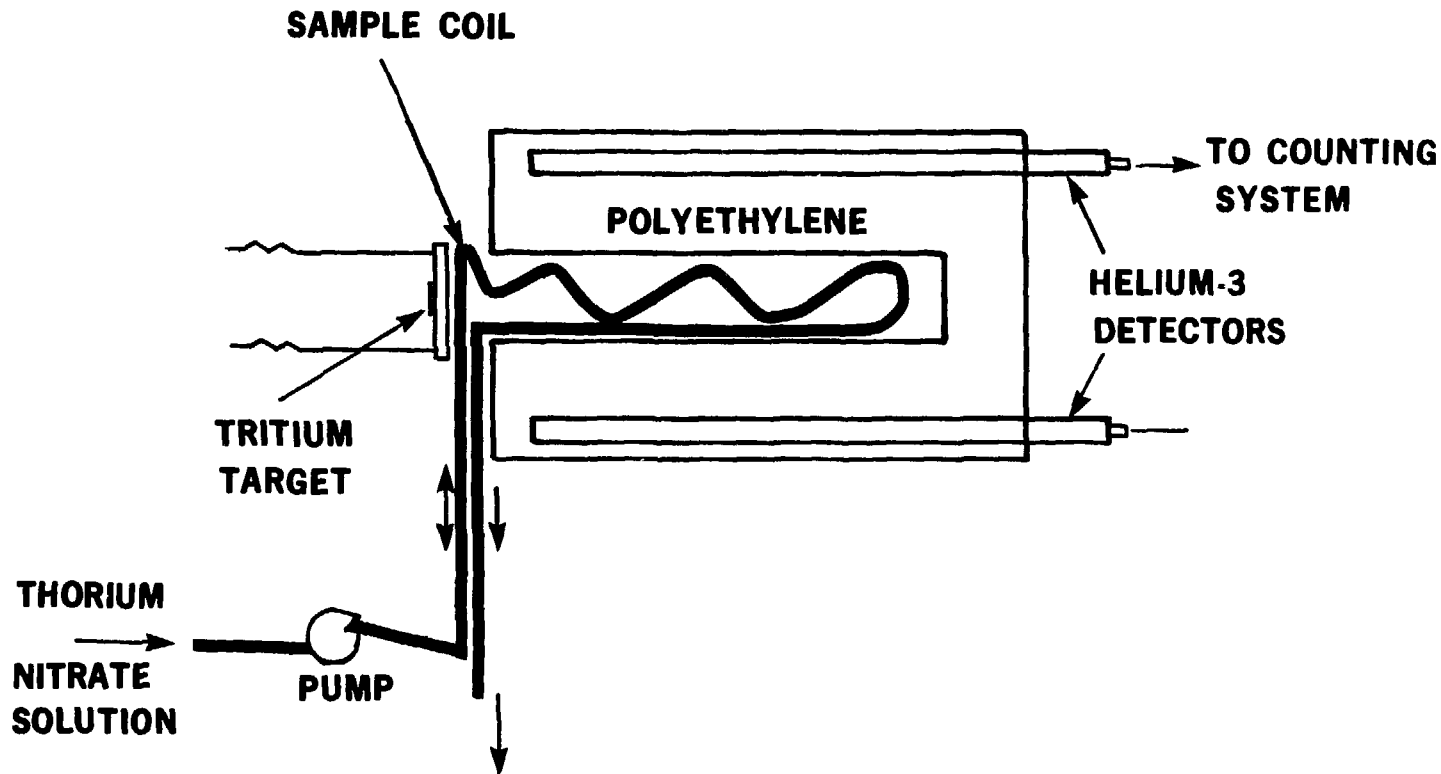


FIGURE 16  
THE EFFECT OF INSERTING POLYETHYLENE BETWEEN NEUTRON  
SOURCE AND SAMPLE FOR THE LARGE WELL DETECTOR



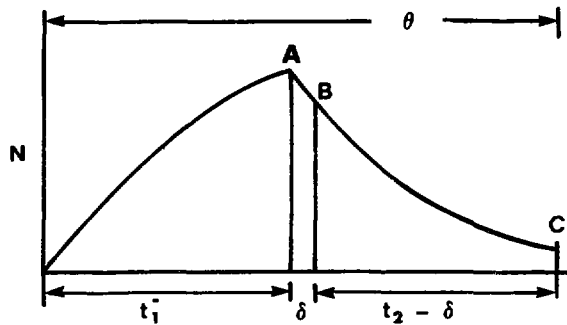
**FIGURE 17**  
**EXPERIMENTAL SYSTEM FOR IRRADIATION OF THORIUM NITRATE STREAMS**

APPENDIX A

CALCULATION OF THE OPTIMUM IRRADIATION TIME

Delayed neutron counting by pulsed neutron irradiation involves the counting and recording of the delayed neutrons emitted between successive irradiations of a fissionable isotope. Figure A-1 illustrates a single irradiation-count cycle showing the activity,  $N$ , produced in a total cycle time of  $\theta$ . The isotope is irradiated with neutrons for  $t_1$  seconds.

FIGURE A-1



A time delay of  $\delta$  is introduced before counting of the delayed neutrons begins, to prevent undesired events entering the counting period. The counting period is  $t_2 - \delta$ . For a complete experiment  $n$  cycles each of duration  $\theta$ , are used for a total experimental time  $T$ .

It is desired to derive an expression for the number of precursors and the number of delayed neutrons present, at any time during a complete cycle. If we consider a precursor group of average decay constant  $\lambda$ , then the induced activity ( $N_A$ ) after irradiation time  $t_1$  is:

$$N_A = K(1 - e^{-\lambda t_1}) \quad (1)$$

After the delay period,  $\delta$ , the activity is:

$$N_B = K(1 - e^{-\lambda t_1})e^{-\lambda \delta} \quad (2)$$

and the activity remaining at the end of the cycle is:

$$N_C = K(1 - e^{-\lambda t_1})e^{-\lambda \delta} e^{-\lambda (t_2 - \delta)} \quad (3)$$

The constant,  $K$ , is a product of the fission rate  $\dot{F}$ , the delayed neutron fraction  $\beta$ , the average total number of fission neutrons,  $\bar{\nu}$ , the relative abundance of delayed neutrons from a precursor group,  $a$ , and the reciprocal of the decay constant of that group, that is:

$$K = \dot{F} \beta \frac{\bar{\nu} a}{\lambda} \quad (4)$$

The fission rate,  $\dot{F}$ , is a function of the incident flux  $\phi$ , the cross section of fission  $\sigma_f$  and the number of atoms of the isotope being irradiated  $N_I$ , thus

$$K = \phi \sigma_f N_I \beta \frac{\bar{\nu} a}{\lambda} \quad (5)$$

The number of delayed neutrons,  $R$ , emitted between B and C is:

$$R = N_B \lambda \int_0^{t_2 - \delta} e^{-\lambda t} dt \quad (6)$$



where  $N_B$  is the activity at point, B, Figure A-1. After integration and substitution of  $N_B$  from (2), equation (6) becomes:

$$R = K(1 - e^{-\lambda t_1})e^{-\lambda \delta} (1 - e^{-\lambda(t_2 - \delta)}) \quad (7)$$

If  $\delta$  is small with respect to  $\theta$ , then  $e^{-\lambda \delta}$  approaches 1. It can be shown that R is a maximum when the irradiation time,  $t_1$ , is equal to the counting time,  $t_2$ . Thus  $t_1 = t_2 = \frac{\theta}{2}$ . Equation 7 now becomes:

$$R = K(1 - e^{-\lambda t_2})2 \quad (8)$$

To apply this equation to any situation a general equation of the delayed neutron decay curve  $D(t)$  must be obtained. In general the yield of delay neutrons may be written as:

$$R = \int_0^t D(t) dt \quad (9)$$

Applying the boundary conditions imposed by Figure A-1

$$R = \int_{\frac{\theta}{2} + \delta}^{\theta} A e^{-\lambda t} dt \text{ where } A \text{ is a constant} \quad (10)$$

Upon integration, equation 10 may be equated to equation 8, and A obtained as:

$$A = \dot{F} \bar{\nu} a \frac{(1 - e^{-\lambda \theta/2})}{e^{-\lambda \theta/2}} \quad (11)$$

In general form of the decay curve can now be deduced as:

$$D(t) = \dot{F} \bar{\nu} a \frac{(1 - e^{-\lambda \theta/2})}{e^{-\lambda \theta/2}} e^{-\lambda t} \quad (12)$$

where  $t$  is the time after the irradiation pulse ceases. The area under the curve for each cycle gives the total delayed neutrons, and when added to those remaining from previous irradiations gives the total yield. The total yield  $R(n,T)$  of delayed neutrons for  $n$  cycles is:

$$R(n,T) = \frac{\beta \bar{a}}{\lambda} (1 - e^{-\lambda T/2n}) (1 - e^{-\lambda(T-\delta)/2n}) \sum_{z=0}^{n-1} (n-z) e^{-\lambda z(T/n+\delta)} \quad (13)$$

Equation (13) gives the theoretical delayed neutron yield from a single delayed neutron precursor group of decay constant,  $\lambda$ . However, as previously stated, the delayed neutron decay curve is composed of many precursors and is normally approximated by six group half-lives, thus equation (13) is modified to accommodate the six groups giving:

$$R(n,T) = \frac{\beta \bar{a}}{\lambda} \left[ \sum_{i=1}^6 \left( \frac{\beta_i \bar{a}_i}{\lambda_i} (1 - e^{-\lambda_i T/2n}) \right) (1 - e^{-\lambda_i(T-\delta)/2n}) e^{-\lambda_i} \sum_{z=0}^{n-1} (n-z) e^{-\lambda_i z T/n} \right] \quad (14)$$

The delayed neutron yield for any fissionable isotope may be computed from this equation using the values of  $\beta$  and  $\lambda$  in Table 1, for any irradiation pulse length,  $\theta/2$ . These values determine the pulse length for the optimum delayed neutron response.



**The International Standard Serial Number**

**ISSN 0067-0367**

**has been assigned to this series of reports.**

**To identify individual documents in the series  
we have assigned an AECL-number.**

**Please refer to the AECL-number when  
requesting additional copies of this document  
from**

**Scientific Document Distribution Office  
Atomic Energy of Canada Limited  
Chalk River, Ontario, Canada  
K0J 1J0**

**PRICE - \$4.00 per copy**